

Light Octet Scalars, a Heavy Higgs and Minimal Flavour Violation

C.P. Burgess,^{1,2} Michael Trott,¹ and Saba Zuberi³

¹ *Perimeter Institute for Theoretical Physics,
31 Caroline St. N., Waterloo ON, N2L 2Y5, Canada.*

² *Dept. of Physics & Astronomy, McMaster University,
1280 Main St. W., Hamilton ON, L8S 4M1, Canada.*

³ *Dept. of Physics, University of Toronto,
60 St. George Street, Toronto ON, M5S 1A7, Canada.*

ABSTRACT: It is widely believed that existing electroweak data requires a Standard Model Higgs to be light while electroweak and flavour physics constraints require other scalars charged under the Standard Model gauge couplings to be heavy. We analyze the robustness of these beliefs within a general scalar sector and find both to be incorrect, provided that the scalar sector approximately preserves custodial symmetry and minimal flavour violation (MFV). We demonstrate this by considering the phenomenology of the Standard Model supplemented by a scalar having $SU_c(3) \times SU_L(2) \times U_Y(1)$ quantum numbers $(\mathbf{8}, \mathbf{2})_{1/2}$ — which has been argued [13] to be the only kind of exotic flavour singlet scalar allowed by MFV that couples to quarks. We examine constraints coming from electroweak precision data, direct production from LEP II and the Tevatron, and from flavour physics, and find that the observations allow both the Standard Model Higgs and the new scalars to be simultaneously light — with masses ~ 100 GeV, and in some cases lighter. The discovery of such light coloured scalars could be a compelling possibility for early LHC runs, due to their large production cross section, $\sigma \sim 100$ pb. But the observations equally allow all the scalars to be heavy (including the Higgs), with masses ~ 1 TeV, with the presence of the new scalars removing the light-Higgs preference that normally emerges from fits to the electroweak precision data.

Contents

1. Introduction	1
2. Theory	3
2.1 The Manohar-Wise model	3
2.1.1 Custodial symmetry	5
2.2 Naturalness issues	6
3. Phenomenology	9
3.1 Fits to Electroweak Precision Data	9
3.1.1 Constraints on Octet scalars	13
3.1.2 Implications for the inferred Higgs mass	15
3.1.3 Implications for the tension between leptonic and hadronic asymmetries	18
3.2 Direct-production constraints from LEP	19
3.3 Tevatron constraints	20
3.3.1 Dijet constraints on the production cross section.	20
3.3.2 Gauge boson decays and Lepton Signatures	22
3.3.3 Constraints from $t\bar{t}$ decays.	24
3.3.4 Constraints from $\bar{b}b\bar{b}b$ decays.	24
3.3.5 Constraints from $\gamma\gamma$ decays.	25
3.4 Flavour constraints reexamined for light scalars	26
4. Conclusions	27
A. EWPD fit	29
B. Renormalization	31
C. Mixing of S_R and S_I	33

1. Introduction

Most physicists believe that new physics beyond the Standard Model (SM) awaits discovery at the LHC, and experiments at the Large Hadron Collider (LHC) will soon probe the weak scale and (hopefully) reveal the nature of whatever new physics lies beyond the Standard Model. Since the Higgs sector is among the least understood in the SM, new scalar physics could well be what is found.

However, to be found at the Tevatron or the LHC, any such new scalar physics should be associated with a comparatively low scale, $\Lambda \sim \text{TeV}$. And because the scale is low, it must be checked that the new physics cannot contribute to processes that are well-measured and agree well with the SM, such as electroweak precision data (EWPD) and flavour-changing neutral currents (FCNCs). This suggests taking most seriously those kinds of new physics that suppress such contributions in a natural way. This can be elegantly accomplished if the effective field theory (EFT) appropriate to low energies obeys approximate symmetries, such as a custodial symmetry $SU(2)_C$ [1, 2, 3] for EWPD and the principle of minimal flavor violation (MFV) [4, 5, 6, 7, 8, 9], which suppresses FCNCs when formulated appropriately [10, 11, 12].

Recently, it was discovered [13] that there are comparatively few kinds of exotic scalars that are flavour singlets and can have Yukawa couplings with SM fermions in a way that is consistent with MFV. The only two possible scalar representations allowed are those of the SM Higgs or octet scalars, respectively transforming under the gauge group $SU(3) \times SU(2) \times U(1)$ as $(\mathbf{1}, \mathbf{2})_{1/2}$ or $(\mathbf{8}, \mathbf{2})_{1/2}$.

In this paper we examine what constraints EWPD¹, flavour physics, and direct production constraints place on this general scalar sector consistent with MFV. To this end we consider the Manohar-Wise model, for which only one $(\mathbf{1}, \mathbf{2})_{1/2}$ scalar and one $(\mathbf{8}, \mathbf{2})_{1/2}$ scalar are present.

Since it is the quality of SM fits to electroweak precision data that at present provide our only direct evidence for the existence of the SM Higgs, it is perhaps not surprising that the existence of a scalar octet can alter the Higgs properties to which such fits point. In particular, the best-fit value of the Higgs mass obtained from SM fits to EWPD is now $96^{+29}_{-24} \text{ GeV}$ [14]. We find that for the Manohar-Wise model, EWPD fits both change the implications for the Higgs mass, and limit the allowed mass range of the extended scalar sector.

We find that when the masses of the Higgs and octet scalars are approximately degenerate, the electroweak fits allow both the Higgs and the octet to be light, with masses $\sim 100 \text{ GeV}$ (or even lighter for some components). Alternatively, agreement with EWPD also allows the octet and the Higgs doublets to be both heavy, with masses $\sim 1 \text{ TeV}$. The Higgs doublet can be heavy and remain consistent with precision fits because its contribution to the relevant observables is partially cancelled by the contribution of the octet doublet. Having such a heavy Higgs without ruining electroweak fits is attractive, as a resolution of the so-called ‘LEP Paradox’ [15]. We find that the precision electroweak fits generically prefer to limit the splittings among some of the octet components, but by an amount that does not require fine tuning of parameters in the potential. (The overall masses of the two multiplets are subject to the usual issues associated with the electroweak hierarchy.)

The plan of this paper is as follows, in Section 2 we review the Manohar-Wise model, and describe its motivation as a general scalar sector that can both allow an approximate custodial symmetry and satisfy MFV. In Section 3 we present our results for the phenomenology of

¹We thank J. Erler for private communication on the recent update to the EWPD fit results related to [14].

the model. In particular, we describe its implications for an EWPD fit, and explore the parameter space that allows both doublets to be either light or heavy. Since the fits prefer a scalar spectrum that is approximately custodially symmetric, we also study loop-induced $SU(2)_C$ breaking, and demonstrate that the allowed parameter space is not fine tuned. This section also describes direct-production constraints on the Higgs and octet scalar, coming from both LEP2 and the Tevatron, and reexamines how previously studied flavour constraints change if the new octets are comparatively light. We find that the octets can pass all these tests, for parameters with scalars that are either light or heavy. Some conclusions are briefly summarized in Section 4.

2. Theory

In this section we recap the main features of the the model, obtained by supplementing the SM with an colour-octet, $SU_L(2)$ -doublet scalar. Particular attention is spent on its approximate symmetries, since these underly the motivation to naturally satisfy FCNC and EWPD constraints.

Motivation for $(\mathbf{8}, \mathbf{2})_{1/2}$ scalars.

Minimal Flavour Violation (MFV) is a framework for having flavour-dependent masses without introducing unwanted flavour changing neutral currents (FCNCs). It assumes all breaking of the underlying approximate $SU(3)_U \times SU(3)_D \times SU(3)_Q$ flavour symmetry of the SM is proportional to the up- or down-quark Yukawa matrices. The fact that only scalars transforming as $(\mathbf{8}, \mathbf{2})_{1/2}$, or as the SM Higgs [13], can Yukawa couple to SM fermions consistent with MFV is the motivation of the phenomenological study we present here.

However, we also note that octet scalars appear in many specific new-physics scenarios, including various SUSY constructions [16, 17], topcolour models [18], and models with extra dimensions [19, 20]. Various approaches to grand unification also have light colour octet scalars, including Pati-Salam unification [21] and $SU(5)$ unification [22, 23, 24]. Colour octet doublets have also recently been used to study new mechanisms for neutrino mass generation [25]. Octet scalar doublets appear naturally in models of the Chiral-Colour [26, 27] type where QCD originates in the chiral colour group $SU_L(3) \times SU_R(3)$, since in this case octet doublets are expected in addition to the Higgs as $\mathbf{3} \otimes \bar{\mathbf{3}} = \mathbf{8} \oplus \mathbf{1}$. As discussed in [28] one can also consider the class of models where the SM is extended with $SU(N) \times SU(3)_C \times SU(2)_L \times U(1)_Y$ and imagine model-building composite Higgs models with a $(\mathbf{8}, \mathbf{2})_{1/2}$ scalar in the low energy spectrum. We emphasize that although many BSM scenarios contain $(\mathbf{8}, \mathbf{2})_{1/2}$ scalars our motivation is essentially phenomenological.

2.1 The Manohar-Wise model

In the Manohar Wise model [13], the scalar sector of the SM is supplemented with the $(\mathbf{8}, \mathbf{2})_{1/2}$

scalar denoted

$$S^A = \begin{pmatrix} S^{A+} \\ S^{A0} \end{pmatrix} \quad (2.1)$$

where A is the colour index.

The Yukawa couplings of the $(\mathbf{8}, \mathbf{2})_{1/2}$ scalar to quarks is determined up to overall complex constants, η_U and η_D , to be

$$L = \eta_U g_{ij}^U \bar{u}_R^i T^A (S^A)^T \epsilon Q_L^j - \eta_D g_{ij}^D \bar{d}_R^i T^A (S^A)^\dagger Q_L^j + h.c., \quad (2.2)$$

where g^U and g^D are the standard model Yukawa matrices, i, j are flavor indices and

$$\epsilon = \begin{pmatrix} 0 & 1 \\ -1 & 0 \end{pmatrix}. \quad (2.3)$$

The most general renormalizable potential [13] is

$$\begin{aligned} V = & \frac{\lambda}{4} \left(H^{\dagger i} H_i - \frac{v^2}{2} \right)^2 + 2m_S^2 \text{Tr} \left(S^{\dagger i} S_i \right) + \lambda_1 H^{\dagger i} H_i \text{Tr} \left(S^{\dagger j} S_j \right) + \lambda_2 H^{\dagger i} H_j \text{Tr} \left(S^{\dagger j} S_i \right) \\ & + \left[\lambda_3 H^{\dagger i} H^{\dagger j} \text{Tr} \left(S_i S_j \right) + \lambda_4 H^{\dagger i} \text{Tr} \left(S^{\dagger j} S_j S_i \right) + \lambda_5 H^{\dagger i} \text{Tr} \left(S^{\dagger j} S_i S_j \right) + h.c. \right] \\ & + \lambda_6 \text{Tr} \left(S^{\dagger i} S_i S^{\dagger j} S_j \right) + \lambda_7 \text{Tr} \left(S^{\dagger i} S_j S^{\dagger j} S_i \right) + \lambda_8 \text{Tr} \left(S^{\dagger i} S_i \right) \text{Tr} \left(S^{\dagger j} S_j \right) \\ & + \lambda_9 \text{Tr} \left(S^{\dagger i} S_j \right) \text{Tr} \left(S^{\dagger j} S_i \right) + \lambda_{10} \text{Tr} \left(S_i S_j \right) \text{Tr} \left(S^{\dagger i} S^{\dagger j} \right) + \lambda_{11} \text{Tr} \left(S_i S_j S^{\dagger j} S^{\dagger i} \right), \quad (2.4) \end{aligned}$$

where i and j are $SU(2)$ indices and $S = S^A T^A$. Since a field redefinition can be used to make λ_3 real, this represents 14 real parameters in the potential beyond those of the SM, which reduce to 9 in the custodial $SU(2)$ symmetric case — see eqs. (2.9) through (2.12), below. No new parameters enter in the couplings of the $(\mathbf{8}, \mathbf{2})_{1/2}$ scalar to the electroweak gauge bosons since it has the same electroweak quantum numbers as the Higgs. We use this fact to bound the masses of the octets in Section 3.1.1. The $\lambda_{1,2,3}$ terms in Eq.(2.4) lift the mass degeneracy of the octet states when the Higgs acquires a vacuum expectation value. Expanding the neutral scalar octet as

$$S^{A0} = \frac{S_R^{A0} + i S_I^{A0}}{\sqrt{2}} \quad (2.5)$$

the tree level masses become [13]

$$\begin{aligned} M_{\pm}^2 &= M_S^2 + \lambda_1 \frac{v^2}{4} \\ M_R^2 &= M_S^2 + (\lambda_1 + \lambda_2 + 2\lambda_3) \frac{v^2}{4} \\ M_I^2 &= M_S^2 + (\lambda_1 + \lambda_2 - 2\lambda_3) \frac{v^2}{4}. \quad (2.6) \end{aligned}$$

2.1.1 Custodial symmetry

We find below that EWPD fits prefer the masses of some of the scalars in these models to be approximately degenerate in mass. In particular, fits prefer a mass pattern that can be naturally understood as being due to an approximate custodial $SU(2)_C$ symmetry, under which the SM vector bosons transform as a triplet and the Higgs transforms as a singlet and a triplet. This symmetry is broken in the SM both by hypercharge gauge interactions, and by the mass splittings within fermion electroweak doublets.

For these reasons we next explore the implications of the custodial-invariant limit, for which $SU(2)_C$ is an exact symmetry of the underlying new physics beyond the SM. In this scenario, it is interesting to examine the case that $SU(2)_C$ is preserved in the Manohar-Wise model potential at a high scale ~ 1 TeV, up to the breaking that must be induced by the SM. Imposing exact $SU(2)_C$ on the octet Higgs potential we find that the potential can be rewritten in terms of bi-doublets

$$\Phi = (\epsilon \phi^*, \phi), \quad \mathcal{S}_A = (\epsilon S_A^*, S_A), \quad (2.7)$$

where ϵ is given in Eqn. (2.3) and the most general gauge- and custodial-invariant potential becomes

$$\begin{aligned} V = & \frac{\lambda}{16} \left[\text{Tr} \left(\Phi^\dagger \Phi \right) - v^2 \right]^2 + \frac{m_S^2}{2} \text{Tr} \left(\mathcal{S}_A^\dagger \mathcal{S}_A \right) + \frac{\lambda_1}{8} \text{Tr} \left(\Phi^\dagger \Phi \right) \text{Tr} \left(\mathcal{S}_A^\dagger \mathcal{S}_A \right), \\ & + a_1 \text{Tr} \left(\mathcal{S}^\dagger \Phi \right) \text{Tr} \left(\mathcal{S}^\dagger \Phi \right) + \left(b_1 \text{Tr}[\text{T}^A \text{T}^B \text{T}^C] \text{Tr} \left(\Phi^\dagger \mathcal{S}_A \mathcal{S}_B^\dagger \mathcal{S}_C \right) + h.c. \right) \\ & + c_1 \text{Tr}[\text{T}^A \text{T}^B \text{T}^C] \text{Tr} \left(\mathcal{S}_A^\dagger \mathcal{S}_C \right) \text{Tr} \left(\mathcal{S}_B^\dagger \Phi \right), \\ & + d_1 \text{Tr}[\text{T}^A \text{T}^B \text{T}^C \text{T}^D] \text{Tr} \left(\mathcal{S}_A^\dagger \mathcal{S}_B \right) \text{Tr} \left(\mathcal{S}_C^\dagger \mathcal{S}_D \right), \\ & + e_1 \text{Tr}[\text{T}^A \text{T}^B] \text{Tr}[\text{T}^C \text{T}^D] \text{Tr} \left(\mathcal{S}_A^\dagger \mathcal{S}_B \right) \text{Tr} \left(\mathcal{S}_C^\dagger \mathcal{S}_D \right), \\ & + f_1 \text{Tr}[\text{T}^A \text{T}^B] \text{Tr}[\text{T}^C \text{T}^D] \text{Tr} \left(\mathcal{S}_A^\dagger \mathcal{S}_C \right) \text{Tr} \left(\mathcal{S}_B^\dagger \mathcal{S}_D \right), \end{aligned} \quad (2.8)$$

where T_A is used as a basis in colour space with 9 independent terms when the potential is $SU(2)_C$ invariant.² Expanding out the potential and comparing to the general result of eq. (2.4), we confirm the result of [13] that $SU(2)_C$ implies

$$2 \lambda_3 = \lambda_2, \quad (2.9)$$

$$2 \lambda_6 = 2 \lambda_7 = \lambda_{11}, \quad (2.10)$$

$$\lambda_9 = \lambda_{10}, \quad (2.11)$$

but we also find the additional constraint³

$$\lambda_4 = \lambda_5^*. \quad (2.12)$$

²An alternative way to obtain this count is to regard $SU(2)_L \times SU(2)_C$ as $SO(4)$, with both \vec{H} and \vec{S}^A transforming as real fields in the 4-dimensional representation. In this case the invariants of the potential can be written $m_S^2 (\vec{S}^A \cdot \vec{S}^A)$, $d_{ABC} (\vec{H} \cdot \vec{S}^A) (\vec{S}^B \cdot \vec{S}^C)$, $f_{ABC} (\vec{H}_i \cdot \vec{S}_j^A \vec{S}_k^B \cdot \vec{S}_l^C) \epsilon^{ijkl}$, $(\vec{H} \cdot \vec{H}) (\vec{S}^A \cdot \vec{S}^A)$, $(\vec{H} \cdot \vec{S}^A) (\vec{H} \cdot \vec{S}^A)$, $(\vec{S}^A \cdot \vec{S}^A)^2$ and the two independent ways of colour-contracting $(\vec{S}^A \cdot \vec{S}^B) (\vec{S}^C \cdot \vec{S}^D)$.

³We thank A Manohar for communication on this point clearing up a subtlety.

Note that this constraint can effect the production mechanism of the octets at Tevatron and LHC. We see in particular that because $SU(2)_C$ symmetry implies $\lambda_2 = 2\lambda_3$, in this limit M_\pm and M_I become degenerate.

2.2 Naturalness issues

In general, even if the scalar potential is required to be custodial invariant at a particular scale, it does not remain so under renormalization due to the presence of custodial-breaking interactions within the SM itself. In this section we compute these one-loop symmetry breaking effects, allowing us to quantify the extent to which the custodial-invariant potential is fine-tuned. To do so we calculate in Feynman gauge and note that ghost fields do not couple to the components of the S doublet. We also neglect goldstone boson contributions to the mass splitting as they come from the $SU(2)_C$ symmetric potential and so therefore cancel out in the mass splittings; not leading to mixing between the S_R and S_I states.

$SU(2)_C$ breaking due to Yukawa corrections

The breaking of $SU(2)_C$ due to Yukawa couplings is straightforward, the requisite diagrams are given by Fig 1.

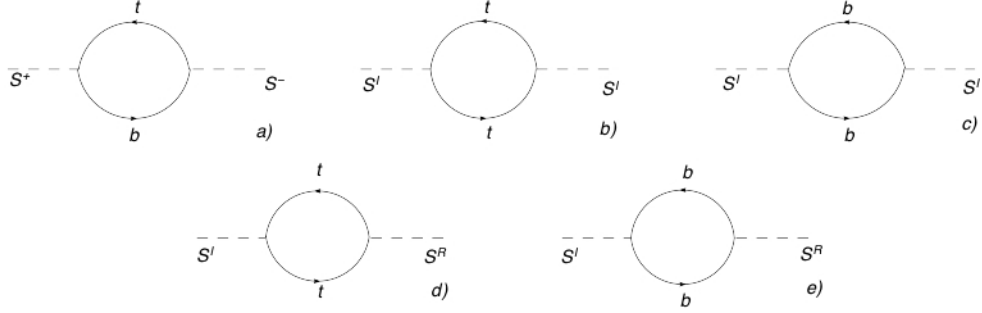


Figure 1: $SU(2)$ violating contributions to S^I, S^\pm masses from the yukawa sector of the theory.

The correction to the mass $S^- S^+$ two point function comes from diagram (a) and is given by

$$\begin{aligned} \delta\langle T\{S^+ S^-\}\rangle_Y &= -\delta_{ab} \frac{(m_b^2 |\eta_D|^2 + m_t^2 |\eta_U|^2)[A_0(m_b^2) + A_0(m_t^2) - p^2 B_0(p^2, m_b^2, m_t^2)]}{16 \pi^2 v^2} \\ &\quad -\delta_{ab} \frac{(m_b^4 |\eta_D|^2 + m_t^4 |\eta_U|^2 + m_b^2 m_t^2 (|\eta_D|^2 + |\eta_U|^2 - 2 \eta_D \eta_U - 2 \eta_D^* \eta_U^*)) B_0(p^2, m_b^2, m_t^2)}{16 \pi^2 v^2} \end{aligned} \quad (2.13)$$

where we express our results in terms of Passarino-Veltman (PV) functions whose definitions are given in [42], and we set $|V_{tb}| \simeq 1$.

The contributions to the S_I^2 operator comes from the diagrams (b) and (c) and is given by

$$\delta\langle T\{S^I S^I\}\rangle_Y = -\delta_{ab} \frac{m_t^2 (2A_0(m_t^2) |\eta_U|^2 + B_0(p^2, m_t^2, m_t^2) (4 m_t^2 \text{Im}[\eta_U]^2 - p^2 |\eta_U|^2))}{16 \pi^2 v^2},$$

$$- \delta_{ab} \frac{m_b^2(2A_0(m_b^2) |\eta_D|^2 + B_0(p^2, m_b^2, m_b^2)(4m_b^2 \text{Im}[\eta_D]^2 - p^2 |\eta_D|^2))}{16 \pi^2 v^2}. \quad (2.14)$$

We are interested in the mass splitting of M_I^2 and M_{\pm}^2 , however to the accuracy we work one can also easily calculate the shifts to $\delta\langle T\{S^R S^R\}\rangle_Y$ and $\delta\langle T\{S^R S^I\}\rangle_Y$ due to the mixing induced between the real and imaginary components of S^{A0} . With these results we can then obtain the contributions to the diagonalized M'_I . The correction to $\delta\langle T\{S^R S^R\}\rangle_Y$ is given by the same diagrams as $\delta\langle T\{S^I S^I\}\rangle_Y$ with the appropriate replacements, giving

$$\begin{aligned} \delta\langle T\{S^R S^R\}\rangle_Y &= -\delta_{ab} \frac{m_t^2(2A_0(m_t^2) |\eta_U|^2 + B_0(p^2, m_t^2, m_t^2)(4m_t^2 \text{Re}[\eta_U]^2 - p^2 |\eta_U|^2))}{16 \pi^2 v^2}, \\ &- \delta_{ab} \frac{m_b^2(2A_0(m_b^2) |\eta_D|^2 + B_0(p^2, m_b^2, m_b^2)(4m_b^2 \text{Re}[\eta_D]^2 - p^2 |\eta_D|^2))}{16 \pi^2 v^2} \end{aligned} \quad (2.15)$$

The mixing of the S_R, S_I fields at one loop $\delta\langle T\{S^R S^I\}\rangle_Y$ is given by diagrams (d,e) and is given by

$$\delta\langle T\{S^R S^I\}\rangle_Y = -\delta_{ab} \frac{(m_b^4 \text{Re}[\eta_D] \text{Im}[\eta_D] B_0(p^2, m_b^2, m_b^2) - m_t^4 \text{Re}[\eta_u] \text{Im}[\eta_U] B_0(p^2, m_t^2, m_t^2))}{4 \pi^2 v^2}$$

which is only nonzero when at least one of the MFV proportionality constants η_D, η_U are imaginary as expected. We define the mixing angle and renormalize the theory in the Appendix.

Gauge sector $SU(2)_C$ violating corrections

Calculating the required four diagrams represented by diagrams (g,i) in Fig 2 one finds

$$\delta\langle T\{S^I S^I\}\rangle_G = \frac{g_1^2}{16\pi^2} \delta^{AB} \left(\frac{dA_0[M_W^2]}{2} + \frac{dA_0[M_Z^2]}{4c_W^2} - \frac{1}{2} I_3[p^2, M_W^2, M_{\pm}^2] - \frac{1}{4c_W^2} I_3[p^2, M_Z^2, M_R^2] \right)$$

where $c_W \equiv \cos[\theta_W]$ and the integral is given in terms of PV functions as follows

$$I_3[p^2, M_a^2, M_b^2] = (2p^2 + 2M_b^2 - M_a^2) B_0[p^2, M_a^2, M_b^2] + 2A_0[M_a^2] - A_0[M_b^2]. \quad (2.16)$$

The result for $\delta\langle T\{S^R S^R\}\rangle_G$ is identical up to the replacement $M_R \rightarrow M_I$. One can similarly calculate the other six diagrams corresponding to (f,h) that give the following contribution for $\delta\langle T\{S^+ S^-\}\rangle_G$ in terms of PV functions⁴

$$\begin{aligned} \delta\langle T\{S^+ S^-\}\rangle_G &= \frac{g_1^2}{16\pi^2} \delta^{AB} \left(\frac{dA_0[M_W^2]}{2} + \frac{d(1 - 2s_W^2)^2 A_0[M_Z^2]}{4c_W^2} - \frac{1}{4} I_3[p^2, M_W^2, M_R^2] \right. \\ &\left. - \frac{1}{4} I_3[p^2, M_W^2, M_I^2] - \frac{(1 - 2s_W^2)^2}{4c_W^2} I_3[p^2, M_Z^2, M_{\pm}^2] - s^2 I_3[p^2, 0, M_{\pm}^2] \right) \end{aligned} \quad (2.17)$$

Mixing between the states S^I, S^R is forbidden in the gauge sector as the couplings are real.

⁴Note that diagram (f) with a photon loop is scaleless and vanishes in dim reg.

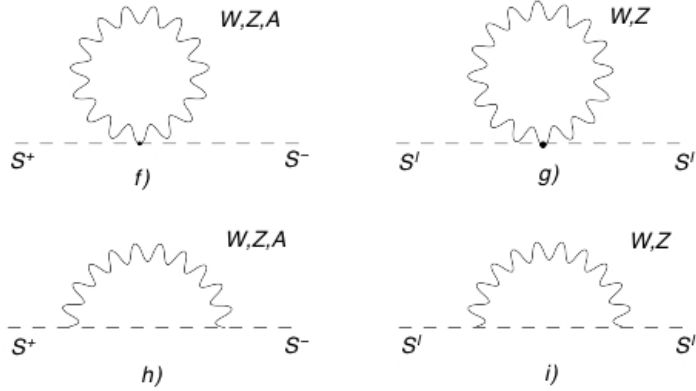


Figure 2: SU(2) violating contributions from the gauge sector of the theory.

Given these loop-generated effects, we wish to estimate how large the custodial-symmetry-breaking interactions are once we run down to observable energies from the scale of new physics. The answer depends on how far we must run, however due to the hierarchy problem of the Higgs mass (which is only accentuated when more light scalars are added to the spectrum), it is likely that new physics must intervene at a relatively low scale for new physics of \sim TeV. Such a low scale for a UV completion implies that the symmetry structure of the UV theory is consistent with EWPD and flavour constraints.

The splitting induced by SM interactions is given by the difference between the renormalized mass at Λ and the low scale, where we ignore the running for simplicity in this estimate

$$\int_{\Lambda}^m \left(\frac{\partial M_i^2}{\partial \mu} \right) \partial \mu = M_i^2 [Z_{Mi}^{\alpha}(\mu = \Lambda) - Z_{Mi}^{\alpha}(\mu = m)], \quad (2.18)$$

where Z_{Mi}^{α} is the leading perturbative correction of the mass counterterms, whose values are given explicitly in the appendix using a zero-momentum subtraction scheme.

As is shown in detail in the next section, the largest M_I, M_{\pm} SU(2)_C violating mass-splitting that is allowed by our EWPD fit is approximately $\sim 40(55)$ GeV for the entire 68%(95%) confidence regions (see Figure 6). We now examine how natural such a small splitting is assuming a typical low mass of 150 GeV.

In determining the splitting, the values of η_i employed are critical. For the lower bound on the η_i we take the one approximate loop radiatively induced value $\eta_i \sim 0.35^2/(16\pi^2)$. Note that we use the result of [40] that determined an upper bound on $|\eta_U|$ from the effect of the octet on $R_b = (Z \rightarrow \bar{b}b)/(Z \rightarrow \text{Hadrons})$. For charged scalar masses of (75, 100, 200) GeV the one sigma allowed upper value for $|\eta_U|$ is (0.27, 0.28, 0.33).

For $M_{\pm} = 150$ GeV, we choose the couplings to give the largest induced splitting consistent with other experimental constraints ($\eta_U = 0.3, \eta_D = 0.45$), $M_I = 150$ GeV (its value before the perturbative correction in the high scale SU(2)_C preserving scenario) and $M_R = (190, 230)$ GeV which are the maximum values consistent with EWPD for the (68%, 95%) re-

gions. We find that the EWPD regions begin to have tuning for a high scale degenerate mass spectrum at (90 TeV, 8000 TeV). Conversely choosing the unknown $\eta_U, \eta_D \sim 0.35^2/(16\pi^2)$ one finds that the (68%, 95%) regions begin to have some degree of tuning for scales of (170 TeV, 19000 TeV). For a UV completion that approximately preserves MFV and $SU(2)_C$, considering a SM and octet low energy scalar mass spectrum allowed by EWPD is not a fine tuned scenario.

3. Phenomenology

We next turn to the various observational constraints. As we shall see, the most robust constraints are those coming from the absence of direct pair-production at LEP, which require

$$M_{\pm} \gtrsim 100 \text{ GeV} \quad \text{and} \quad M_R + M_I \gtrsim 200 \text{ GeV}. \quad (3.1)$$

Since the octet scalar couples to both photons and gluons, these constraints are essentially kinematic up to the highest energies probed by LEP (more about which below).

3.1 Fits to Electroweak Precision Data

A strong restriction on the properties of exotic scalars comes from precision electroweak measurements, whose implications we now explore in some detail. The dominant way that such scalars influence the electroweak observables is through their contributions to the gauge boson vacuum polarizations; the so-called ‘oblique’ corrections [31, 32, 33]. The calculation of the oblique corrections proceeds as usual with the vacuum polarizations being determined directly by evaluating the diagrams given in Figure 3.

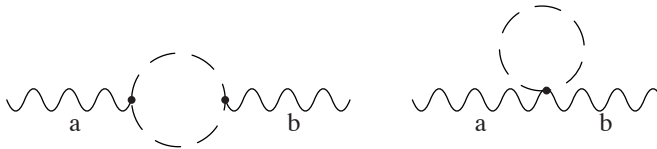


Figure 3: Self energies calculated for the EWPD constraints on the octets, where $(a, b) = (W^+W^-, ZZ, \gamma\gamma, Z\gamma)$. The self energies needed to determine STUVWX are given in the Appendix.

When evaluating these it is important to keep in mind that the direct production constraints, eq. (3.1), can allow one of M_R or M_I to be significantly lower than 100 GeV. This is important because it precludes our using the most commonly-used three-parameter (S, T and U) parametrization of the oblique corrections [31, 32, 33], since these are based on expanding the gauge boson vacuum energies out to quadratic order: $\Pi_{ab}(q^2) \simeq A_{ab} + B_{ab}q^2$, where a and b denote one of Z , W or γ . Since the electroweak precision measurements take place at $q^2 \simeq 0$ or $q^2 \simeq M_Z^2$, using the quadratic approximation for $\Pi_{ab}(q^2)$ amounts to neglecting contributions that are of relative order M_Z^2/M^2 , where M is the scale associated with the new physics of interest (in our case the new-scalar masses). This approximation becomes inadequate for M below 100 GeV, and so we must instead use the full 6-parameter description

(STUVWX), such as in the formalism of ref. [29, 30]. In general, the STUVWX formalism reduces to the three-parameter STU case when all new particles become very heavy.

For ease of comparison with past results we start by quoting the results we obtain for the fit to the six parameters of the STUVWX oblique formalism, regardless of how they depend on the parameters of the Manohar-Wise model. The results are given in Table 1, which compares the results obtained by fitting 34 observables (listed in an appendix) to (i) all six parameters (STUVWX); (ii) only three parameters (STU); or just two parameters (ST). The number of degrees of freedom in these fits to (6, 3, 2) parameters is $v = (28, 31, 32)$, respectively. The χ^2/v for the three fits is within one standard deviation $\sqrt{2/v} = (0.27, 0.25, 0.25)$ of the mean of 1, indicating a good quality of fit. The experimental values and theoretical predictions used are given in Table 2 in the Appendix.

Oblique	STUVWX Fit ($\chi^2/v = 0.91$)	STU Fit ($\chi^2/v = 0.99$)	ST Fit ($\chi^2/v = 0.98$)
S	0.07 ± 0.41	-0.02 ± 0.08	$-9.9 \times 10^{-3} \pm 0.08$
T	-0.40 ± 0.28	-0.02 ± 0.08	$1.1 \times 10^{-2} \pm 0.07$
U	0.65 ± 0.33	0.06 ± 0.10	-
V	0.43 ± 0.29	-	-
W	3.0 ± 2.5	-	-
X	-0.17 ± 0.15	-	-

Table 1: EWPD Fit Results in various schemes for the 34 observables listed in the Appendix. The STU and ST fits fix the other oblique corrections to zero as a prior input. The error listed is the square root of the diagonal element of the determined covariance matrix. The central values of the fitted oblique corrections decrease as more parameters are turned off. All three fits are consistent with past results and the PDG quoted fit results.

The correlation coefficient matrix for the three fit results are as follows,

$$M_{STUVWX} = \begin{pmatrix} 1 & 0.60 & 0.38 & -0.57 & 0 & -0.86 \\ 0.60 & 1 & -0.49 & -0.95 & 0 & -0.13 \\ 0.38 & -0.49 & 1 & 0.46 & -0.01 & -0.76 \\ -0.57 & -0.95 & 0.46 & 1 & 0 & 0.13 \\ 0 & 0 & -0.01 & 0 & 1 & 0 \\ -0.86 & -0.13 & -0.76 & 0.13 & 0 & 1 \end{pmatrix}, \quad (3.2)$$

$$M_{STU} = \begin{pmatrix} 1 & 0.84 & -0.20 \\ 0.84 & 1 & -0.49 \\ -0.20 & -0.49 & 1 \end{pmatrix}, \quad M_{ST} = \begin{pmatrix} 1 & 0.87 \\ 0.87 & 1 \end{pmatrix}. \quad (3.3)$$

We use the results of this fit to constrain the masses allowed in the Manohar-Wise model by computing the vacuum polarizations as functions of the masses of the octet and Higgs

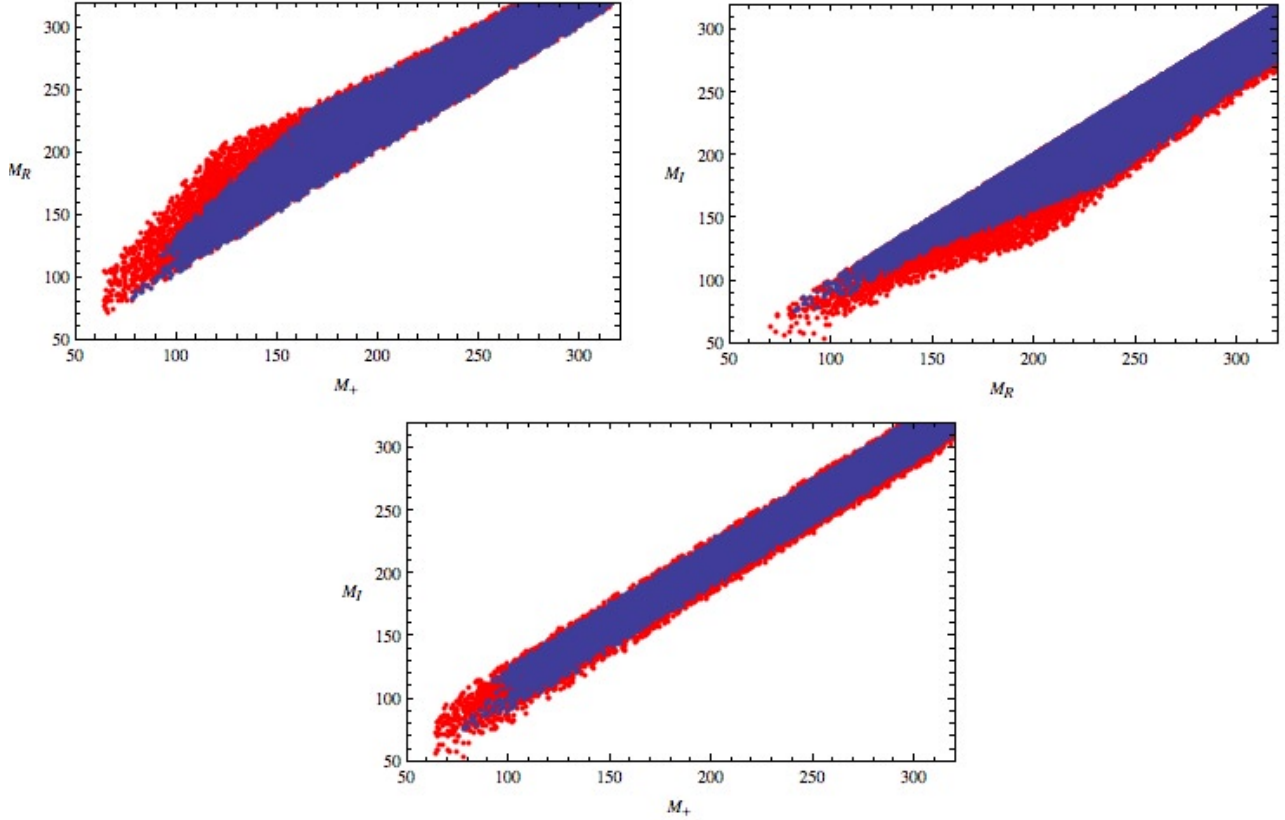


Figure 4: Comparison of the three and six parameter fits for low masses. (The upper two panels are not symmetric about $M_I = M_R$ and $M_R = M_+$ because we scan only through positive values for the couplings, λ_i .) The three parameter fit is red (grey) and the six parameter fit is blue (black). Contrary to naive expectations the six parameter fit is more constraining on the model despite the extra parameters; the correlations between the extra parameters (S, X and U, X and T, V) increases the constraints on the model. The masses are in GeV. EWPD constrains the mass spectrum to be approximately $SU(2)_C$ symmetric in either case where $M_{\pm} \approx M_I$.

scalars. We obtain allowed mass ranges for the scalars by demanding that the contribution of the new physics (and the difference between the floating Higgs mass and its fiducial value, which we take from the SM best fits to be 96 GeV), $\Delta\chi^2$ which satisfies

$$(\mathcal{C}^{-1})_{i,j}(\Delta\theta_i)(\Delta\theta_j) < 7.0385 (12.592) \quad (3.4)$$

for the 68% (95%) confidence regions defined by the cumulative distribution function for the six parameter fit. Here \mathcal{C} is the covariance matrix constructed from the correlation coefficient matrix given in eq. (3.2) or (3.3)

$$(\mathcal{C}^{-1})_{i,j} = \frac{1}{2} \frac{\partial^2 \chi^2(\theta)}{\partial \theta_i \partial \theta_j} \Big|_{\theta_i = \hat{\theta}_i} \quad (3.5)$$

and $\Delta\theta_i = A_i - A_i^{fit}$ is the difference in $A_i = S, T, U, V, W, X$ as a function of octet masses and the best fit value, given in Table 1.

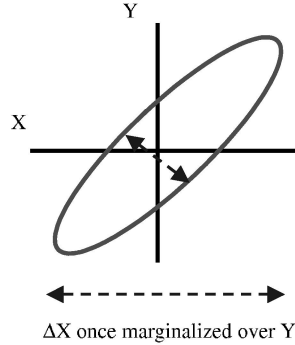


Figure 5: A cartoon of the best-fit confidence interval for a strongly correlated pair of variables, indicating how the best constraints can be missed once one of the variables is marginalized.

An example of the best-fit regions for the allowed octet masses is given in Figure 4, which compares the quality of the constraints that are obtained using the full six-parameter (STUVWX) parametrization, as opposed to the three-parameter (STU) expression. The three panels plot the masses of the components of the octet that lie within the 68% confidence ellipsoid of the best-fit value as the various scalar couplings, λ_i , are varied. The two panels of this plot show how these masses are correlated by the condition that the predictions agree with the precision electroweak measurements, and the points in the upper two panels all satisfy $M_I \leq M_R$ and $M_+ \leq M_R$ because we choose to scan only through positive values of the couplings λ_i .

The strongest correlation is between M_I and M_+ , for which agreement with EWPD demands these two masses cannot be split by more than about 50 GeV. This is as might be expected given that this difference must vanish in the limit that the potential is custodial invariant. The breaking of $SU(2)_C$ generically leads to bad fits because custodial-breaking quantities like the parameter $\rho - 1 = \alpha T$ are measured to be very small. New sources of $SU(2)_C$ breaking are extremely constrained, the deviation of the ρ parameter from its SM value is given by $\rho_0 = 1.0004_{-0.0004}^{+0.0008}$ [39].

The comparison in Figure 4 also shows that the six-parameter STUVWX fit agrees with the three-parameter STU fit when all scalars are heavy, as might be expected. It also shows that the six-parameter fit is the more constraining one when the octet masses are light. We understand that this happens because of the strong correlations amongst the oblique

parameters, which implies that the best-constrained parameter direction is not aligned along any of the STUVWX axes, as shown in Figure 5. As a result the constraint obtained by restricting to the axes $V = W = X = 0$ can be weaker than the full result, significantly affecting the determined 68% confidence regions. For this reason our remaining results quote only the results of the full six-parameter fit.

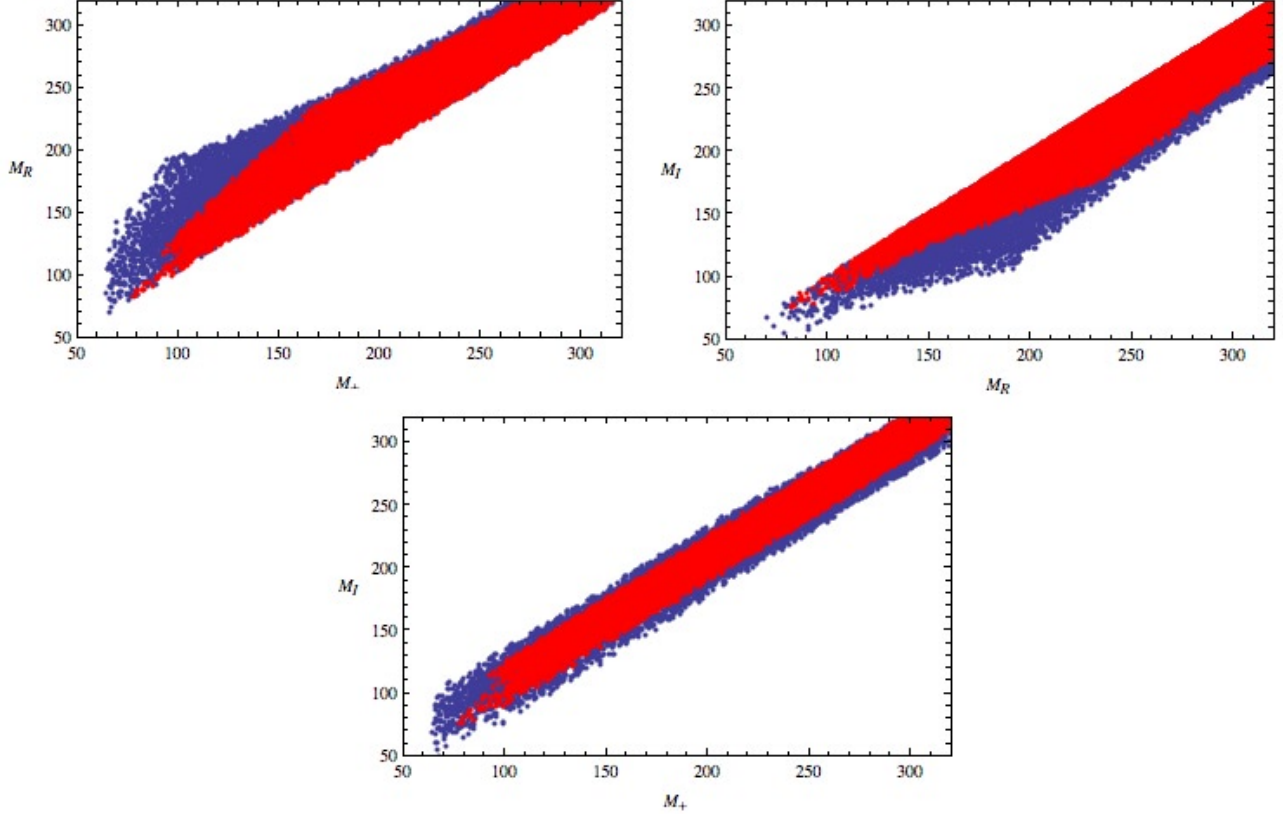


Figure 6: Comparison of the 68% red (grey) and 95% blue (black) confidence regions when $0 < \lambda_i < 1$. The masses are in GeV, and $M_I, M_+ \leq M_R$ because we scan only through positive values of the couplings λ_i . For low masses the 95% confidence region is significantly expanded compared to the 68% region, this is due to the spread of available masses being larger for low masses, as the mass splitting between the states scales as $\sim v^2/m_s$. We examine the naturalness of this mass spectrum in Section 2.2 and find that it is not simply a fine tuned solution for an underlying new physics sector.

3.1.1 Constraints on Octet scalars

Figure 6 displays the 68% and 95% confidence regions of the model for couplings that range through the values $0 < \lambda_i < 1$, while Figure 7 does the same for couplings that run through the larger range $0 < \lambda_i < 10$, where $i = 1, 2, 3$. As noted above, agreement with the EWPD selects an approximately $SU(2)_C$ symmetric mass spectrum, where $\lambda_2 \approx 2\lambda_3$ and $|M_{\pm} - M_I| < 50 \text{ GeV}$, but this is easily understood. Consider the case where the octets are

heavy, $v^2/M_S^2 \ll 1$, which was examined in [13]. In this mass regime it is the model that constrains the mass spectrum to be degenerate, $M_{\pm} \approx M_R \approx M_I$, since the mass splittings scale as v^2/M_S from Eq. (2.6). The contribution of the octets to the S and T parameters,⁵ is then [13]

$$S = \frac{\lambda_2 v^2}{6 \pi M_S^2}, \quad T = \frac{v^4}{96 \pi^2 M_S^2 s_W^2 M_W^2} (\lambda_2^2 - (2 \lambda_3)^2), \quad (3.6)$$

where $s_W \equiv \sin(\theta_W)$. Large corrections to S and T are avoided if λ_i decreases and preserves approximate $SU(2)_C$ as M_S decreases, therefore allowing smaller octet masses.

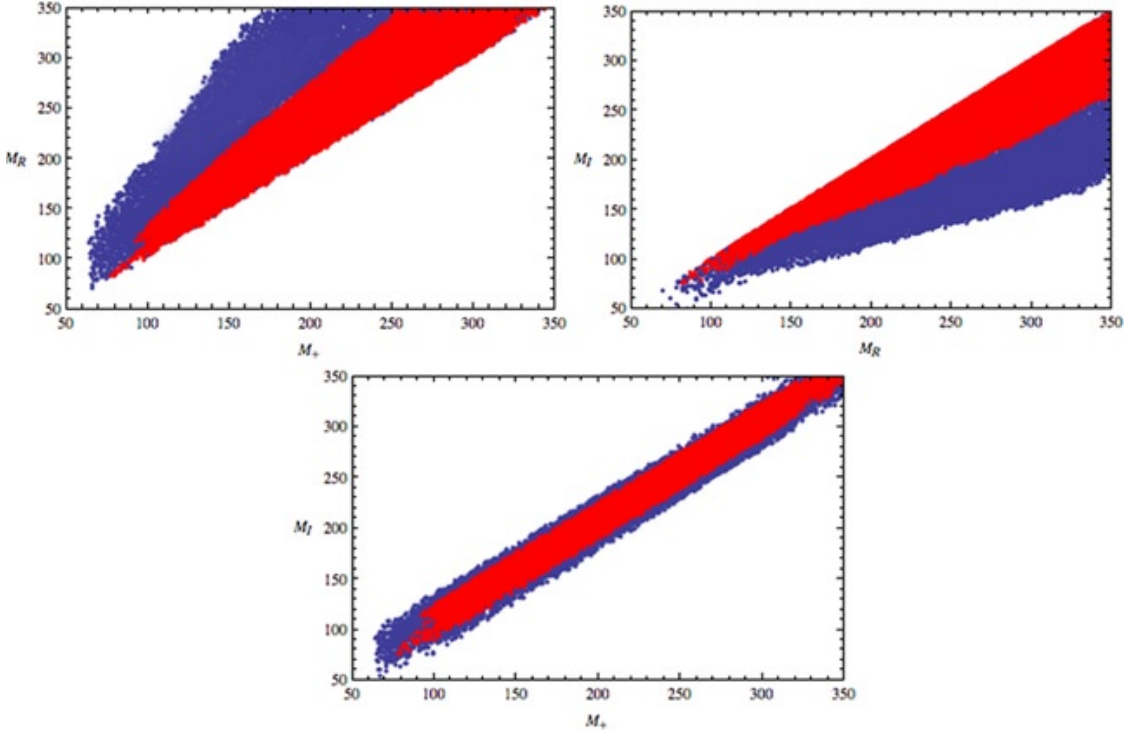


Figure 7: Comparison of the 68% red (grey) and 95% blue (black) confidence regions when $\lambda_i < 10$. Notice that the region selected for by EWPD for $M_I \approx M_+$ that is approximately $SU(2)_C$ symmetric is not enlarged.

How natural are the small intra-octet splittings favoured by EWPD? If the mass splitting is induced by the potential, while $v \gg M_S$, for the octet masses to be allowed by EWPD that selects for a mass degeneracy $\Delta M = M_I - M_{\pm}$, one would have to require that the couplings the the octet-Higgs potential satisfy the scaling rule

$$\lambda_2 - 2\lambda_3 \ll 4 \frac{\Delta M}{v} \sqrt{\lambda_1}. \quad (3.7)$$

⁵We have checked that our results in the STUVWX formalism reduce to these results when $v^2/M_S^2 \ll 1$.

As EWPD requires $\Delta M \sim 50 \text{ GeV}$ for the 95% confidence region this is a mild hierarchy of couplings given by $\lambda_2 - 2\lambda_3 \ll 0.8 \sqrt{\lambda_1}$. Conversely for the case $m_S \gg v$, one requires that the couplings the the octet-Higgs potential satisfy the scaling rule

$$\lambda_2 - 2\lambda_3 \ll 8 \frac{(\Delta M) m_S}{v^2}, \quad (3.8)$$

which is easily satisfied for small λ_i (which we see below are favoured by Landau pole constraints).

The calculations presented in previous sections for the running of custodial-breaking couplings can be used to frame a criteria as to whether the above coupling pattern is natural. The scale dependence of the masses is used to estimate what the $SU(2)_C$ splitting of the masses should be in the theory below the UV scale, Λ , without tuning. One determines how high the scale Λ can be before the EWPD mass regions are excluded. This quantifies the degree of fine tuning of the masses for this scenario.⁶ Since the electroweak hierarchy problem argues that the scale of new physics is likely not too much larger than the TeV regime, we find that the favoured mass splittings are natural, provided that the underlying theory approximately preserves MFV and $SU(2)_C$.

The above ranges of allowed splittings amongst scalar masses directly constrain the three couplings $\lambda_{1,2,3}$ to be small. But small λ_i , for $i \geq 4$, are also favoured due to considerations of the effect of these λ_i on the running of the Higgs self coupling [28]. The mild assumption that one not encounter a Landau pole while running the Higgs self coupling up to 10 TeV, when one assumes $\lambda_{i \geq 4} = 0$ and $m_h = 120 \text{ GeV}$, gives the constraints [28]

$$\lambda_1 \lesssim 1.3, \quad \sqrt{\lambda_1^2 + \lambda_2^2} \lesssim 2.2. \quad (3.9)$$

However, generically $\lambda_{i \geq 4} \neq 0$ and if the octets and the Higgs were part of a new sector then the cut-off scale could be lower than 10 TeV. For these reasons we only take these constraints to inspire the $\lambda_i < 1$ limit for the parameter space searches in Figure 6, but also examine parameter space where we relax this bound to $\lambda_i < 10$ in Figure 7. We emphasize that direct production bounds on the octets that rely on their fermionic decays essentially constrain the MFV proportionality factors η_i , while EWPD is complementary in that it constrains the parameters in the potential, λ_i , by constraining the mass spectrum.

3.1.2 Implications for the inferred Higgs mass

Adding the new octet scalar to the SM also affects the best-fit value of the Higgs mass that emerges from fits to EWPD. In particular, we now show that the presence of the octet can remove the preference of the data for a light Higgs, even if the new octet scalar is also heavy.

⁶To determine the mass splitting, we technically need to diagonalize the S_I field which mixes at one loop with S^R . As the non diagonal terms in the mass matrix are one loop, the effects of this diagonalization on the mass eigenstate S'_I shifts the mass at two loop order. See the Appendix for a determination of the mixing angle. Thus to one loop order one can just take the one loop corrections to M_I and M_{\pm} of the last two sections, properly renormalized, to determine the mass splitting through the counterterms.

To determine this effect we calculate the one-loop Higgs contribution to the six oblique parameters and jointly constrain the Higgs mass and the octet masses in the fit. For example, S in this case becomes

$$S = S_{oct}(M_R, M_I, M_{\pm}) + S_{Higgs}(M_h) - S_{Higgs}(M_h = 96 \text{ GeV}) \quad (3.10)$$

where $S_{oct(Higgs)}$ is the one-loop octet (Higgs) contribution to the S parameter. We neglect the two-loop dependence on the Higgs mass in the fit and this leads to an underestimate of the allowed parameter space, as we find the 68% (95%) confidence level values of fitting the Higgs mass alone are given by 112 (160) GeV. This gives a conservative range when comparing to the various allowed values that are strongly dependent on the priors used in the PDG .

The effect of the octets changes the preferred Higgs mass significantly, and two mechanisms are at work depending on the size of the octet mass. If the octet mass M_I is small, it can allow the Higgs mass to increase by effectively replacing it in the oblique loops, thereby giving agreement with EWPD. This is illustrated in the upper-left plot of Figure 8, which shows how a large Higgs mass correlates with small M_I .

The other panels of Figure 8 reveal another mechanism at work, however ⁷. In these one sees that as the upper limit on λ_i is increased, the upper limit on the Higgs mass confidence regions becomes significantly relaxed. This is due to a cancellation between the effects of the heavy octet and the Higgs in their contributions to oblique parameters, that is made possible by a positive ΔT contribution that the octets give to χ^2 . For the three-parameter fit, the χ^2 test is of the form

$$(\mathcal{C}^{-1})_{i,j}(\Delta\theta_i)(\Delta\theta_j) = 596 (\Delta S)^2 - 1159 (\Delta S)(\Delta T) + 751 (\Delta T)^2 \quad (3.11)$$

where we neglect contributions that are not logarithmically sensitive to the Higgs mass at one loop, since this is all that is relevant to the argument. For the three-parameter fit, the 68% confidence region is defined by $(\mathcal{C}^{-1})_{i,j}(\Delta\theta_i)(\Delta\theta_j) < 3.536$ and is easily satisfied for light Higgs masses. As the Higgs mass grows, its contribution to (ΔS) and (ΔT) becomes dominated by the logarithmic dependence

$$(\Delta S) \simeq \frac{\alpha}{12\pi} \log\left(\frac{M_H^2}{\hat{M}_H^2}\right) \quad \text{and} \quad (\Delta T) \simeq -\frac{3\alpha}{16\pi} \log\left(\frac{M_H^2}{\hat{M}_H^2}\right), \quad (3.12)$$

where \hat{M}_H is the reference value of the Higgs mass, which for our fit is 96 GeV. The crucial point is that (ΔT) is negative for $M_H > \hat{M}_H$ and for the SM this quickly excludes large Higgs masses because of the sign flip in the $(\Delta S)(\Delta T)$ term in χ^2 .

Including the contribution of the octets in the large mass regime ($v^2/M_S^2 \ll 1$) modifies these expressions to

$$(\Delta S) \simeq \frac{\alpha}{12\pi} \log\left(\frac{M_H^2}{\hat{M}_H^2}\right) + \frac{\lambda_2 v^2}{6\pi M_S^2},$$

⁷Note that we expect a careful study of the non oblique Higgs and octet mass dependence of R_b will further constrain this parameter space with all scalars heavy but not remove it.

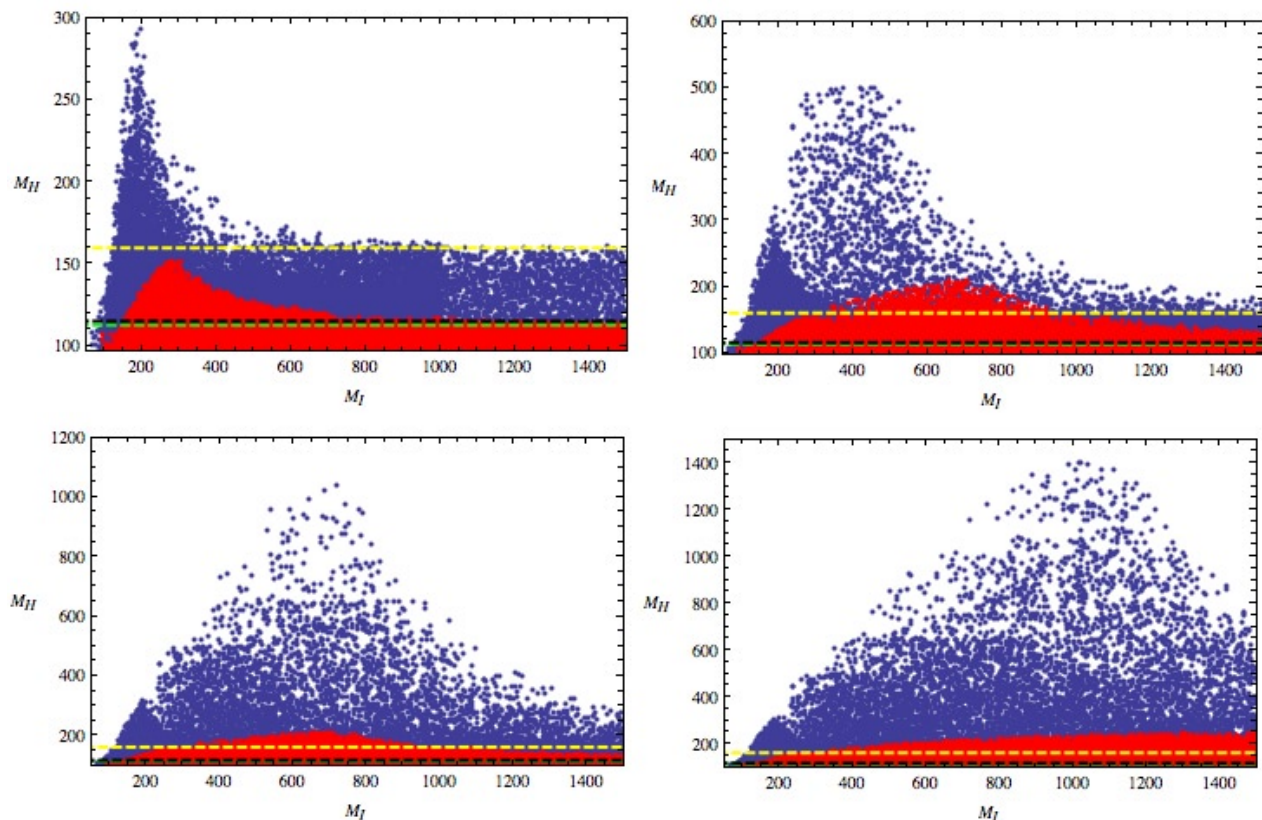


Figure 8: The effect of octets on the fitted value of the Higgs mass. The plots of M_h versus the other octet states are substantially the same. The green line is the 68% confidence bound where the Higgs alone is varied at one loop. The yellow line is the 95% confidence bound where the Higgs alone is varied at one loop, and the black line is the direct production bound on the Higgs mass at 95% confidence. The red (grey) region is the 68% confidence region, while the blue (black) region is the (95%) confidence region for a joint fit to the octets and the Higgs. Notice the increase in vertical scale for the diagrams as the upper limit of the λ_i is increased through 1 (upper left), 3 (upper right), 6 (lower left) and 10 (lower right). The mechanism that is allowing the Higgs mass to increase and still be in agreement with EWPD is the positive ΔT contribution from the octets that is discussed in Section 3.1.2.

$$(\Delta T) \simeq -\frac{3\alpha}{16\pi} \log\left(\frac{M_H^2}{\hat{M}_H^2}\right) + \frac{v^4}{96\pi^2 M_S^2 s_W^2 M_W^2} (\lambda_2^2 - (2\lambda_3)^2), \quad (3.13)$$

where the factor $\lambda_2^2 - (2\lambda_3)^2$ comes from a factor of $(M_R^2 - M_\pm^2)(M_I^2 - M_\pm^2)$ in the octet contribution, and is a measure of the total mass splitting in the doublet. For $\lambda_i > 0$, we know $M_R^2 > M_\pm^2$ and so the octets give a positive contribution to (ΔT) so long as $M_I^2 > M_\pm^2$. The octets (or any other doublet with gauge couplings and small mass splittings) then allow (ΔT) in Eqn. 3.13 to be positive, and so allow a large degree of cancellation between the $(\Delta S)^2$, $(\Delta T)^2$ and $(\Delta S)(\Delta T)$ terms in Eqn. 3.11. The size of the positive (ΔT) contribution

scales with the upper limit on λ_i , explaining the significant relaxation of the Higgs mass bound in Figure 8. We find that the Higgs and the octet scalars could both have masses ~ 1 TeV and still lie within the 95% contour mass region allowed by EWPD. We also note that we restrict our searches to positive λ_i (which must be so for at least some of the couplings to ensure the absence of runaway directions in the potential), however clearly negative λ_2 could also act to relax the EWPD bound on the Higgs mass by giving a negative contribution to (ΔS) .

We emphasize the generic nature of the mechanism, wherein the contributions of TeV scale new physics can mask the contributions of a heavy Higgs to electroweak precision observables. It applies in particular when EW symmetry breaking leads to a mass splitting of an extra SU(2) doublet, since the extra doublet can give a positive contribution to (ΔT) proportional to the mass splittings of the doublet components. This has been recognized as a simple way to raise the EWPD bound on the Higgs mass by satisfying the positive (ΔT) criteria of [35]. Expressed as an effect on the ρ parameter, it also has a long history going back to observations by Veltman [34], being rediscovered for two-Higgs-doublet models in [36], and used for the construction of the Inert Two Higgs doublet (IDM) model [37].⁸ In this latter model, the Higgs mass is raised, addressing the "LEP paradox", and the naturalness of the SM Higgs sector is also improved by raising the cutoff scale of the modified SM. In the IDM model a parity symmetry is imposed to avoid FCNC's.

We note that the example of the general scalar sector consistent with flavour constraints, the Manohar-Wise model examined in this paper, naturally has a number of the benefits of models like the IDM while avoiding the imposition of a parity symmetry. Allowing the second doublet to couple to quarks improves its potential for detection, without introducing large FCNCs due to MFV. It is interesting that the effect of raising the Higgs mass has emerged naturally from the most general MFV scalar sector and was not a model building motivation of the MW model. Variants of the MW model, can address the naturalness of the scalar sector through raising the cut off scale and further the colour charge of the octet provided some rationale for the second doublet not obtaining a vev , through the avoidance of the spontaneous breaking of colour. Also, for the entire parameter range, octets skew the distribution of the allowed Higgs masses so that the direct production bound on the Higgs mass and the EWPD fit of the Higgs mass can be in better agreement.

3.1.3 Implications for the tension between leptonic and hadronic asymmetries

Although the SM produces a good quality global fit to EWPD, there exists a mild tension in the data between the leptonic and hadronic asymmetries. In particular A_{FB}^b deviates from the SM prediction by 2.5σ and favours a heavy Higgs ~ 400 GeV, while A_e differs from the SM by $\sim 2\sigma$ and favours a Higgs mass far below the direct production bound. Here we address the question of whether the oblique contributions of octet scalars can change this tension.

To this end we calculate χ^2 for the hadronic asymmetries A_{FB}^b , A_{FB}^c , A_b , A_c , and for the leptonic asymmetries using A_τ and the A_e values given in Table A. The results are shown

⁸For a similar construction see [38]

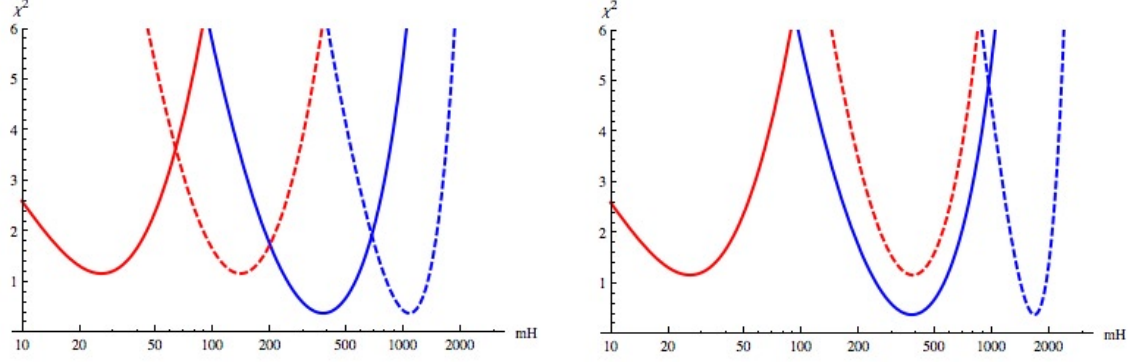


Figure 9: The χ^2 of the leptonic asymmetries (red) and hadronic asymmetries (blue) as a function of Higgs mass in GeV. The solid curves show the contribution of the Higgs alone and the dashed curves are for the Higgs and the octets. The figure on the left is for octet masses $(M_{\pm}, M_R, M_I) = (300, 400, 330)$ GeV and on the right is for $(M_{\pm}, M_R, M_I) = (900, 1000, 940)$ GeV.

in Figure 9, where the solid curves plot χ^2 with the SM Higgs alone and the dashed curves include the octets for a particular mass spectrum allowed by EWPD. The two panels compare results for relatively light and relatively heavy octet scalars.

The figure shows that the preferred value of the Higgs mass is strongly dependent on the mass splitting of the octets. As discussed in Section 3.1.2, the octets, unlike the Higgs, give a positive contribution to ΔT , which depends on the mass splitting in the doublet. This increases the allowed value of the Higgs mass. The octets can change the pull of A_e , for example, to favour large Higgs masses, however they also do the same to A_{FB}^b . As can be seen from Figure 9, although the leptonic and hadronic asymmetries can now both prefer a Higgs masses above the direct production bound of 114.4 GeV, they are not brought in to closer agreement in their predictions for the value of M_H .

We see from this that the octet oblique contributions do not in themselves remove the tension between the leptonic and hadronic asymmetries. However, because the octets are coloured it is possible that their non-oblique corrections to A_{FB}^b might be able to bring together the leptonic and hadronic observables. We leave this observation to a more complete calculation, which lies beyond the scope of this paper.

3.2 Direct-production constraints from LEP

The octets would have been directly produced at LEP2 if they were light enough through the processes in Figure 10.

The production cross sections are given by

$$\begin{aligned} \sigma_{S+S^-} &= \frac{d_A}{4} \left(\frac{4\pi\alpha^2}{3s} \right) \lambda^{3/2} \left(1, \frac{M_+^2}{s}, \frac{M_-^2}{s} \right) \\ &\times \left\{ 1 + 2v_+ v_e \text{Re} \left[\left(1 - \frac{M_Z^2}{s} + \frac{iM_Z\Gamma_Z}{s} \right)^{-1} \right] + v_+^2 (v_e^2 + a_e^2) \left| 1 - \frac{M_Z^2}{s} + \frac{iM_Z\Gamma_Z}{s} \right|^{-2} \right\}, \end{aligned} \quad (3.14)$$

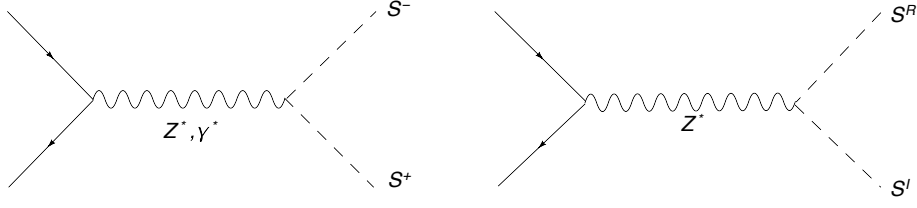


Figure 10: The tree level production mechanism for $S^+ + S^-$ and $S_R^0 + S_I^0$ at LEP II.

$$\sigma_{S_R^0 S_I^0} = \frac{d_A}{4} \left(\frac{4\pi\alpha^2}{3s} \right) \lambda^{3/2} \left(1, \frac{M_R^2}{s}, \frac{M_I^2}{s} \right) v_0^2 (v_e^2 + a_e^2) \left| 1 - \frac{M_Z^2}{s} + \frac{iM_Z\Gamma_Z}{s} \right|^{-2}, \quad (3.15)$$

where we have defined $d_A = 8$, $a_e = -(4s_W c_W)^{-1}$

$$\lambda(x, y, z) = x^2 + y^2 + z^2 - 2xy - 2xz - 2yz, \quad (3.16)$$

$$v_+ = \frac{s_W^2 - c_W^2}{2s_W c_W}, \quad v_0 = \frac{1}{2s_W c_W}, \quad v_e = \frac{-1 + 4s_W^2}{4s_W c_W} \quad (3.17)$$

The highest COM energy at which LEP2 operated was $\sqrt{s} = 209$ GeV, where approximately $\int \mathcal{L} dt \sim 0.1 \text{ fb}^{-1}$ of integrated luminosity was collected. We give a rough estimate of the sensitivity of LEP2 to light octets by requiring less than 10 total events for a given set of masses, $\sigma \times \int \mathcal{L} dt < 10$. Note that these limits are essentially kinematic limits for production, and more accurate exclusions in the mass parameter space are possible, but these will be dependent on the detailed decays of the octets and SM backgrounds and be weaker constraints. The LEP2 production bounds are shown in Figure 11.

3.3 Tevatron constraints

3.3.1 Dijet constraints on the production cross section.

Heavy octet production via gluon fusion has been examined in some detail in the literature see [13, 40, 27]. We use the results of [13, 40, 27] to determine the production cross sections for light octets and consider the relevant bounds on the model in this region from the Tevatron. The single production cross section we use, [40], neglects for simplicity the scalar mass splitting and assumes that η_U , λ_4 and λ_5 are real. However, note that this is partially justified for light masses as EWPD selects for an approximately degenerate mass spectrum with an approximate $SU(2)_C$ symmetry in the underlying potential, giving $\lambda_4 = \lambda_5^*$ and one need only assume one of the couplings are real.⁹ For the sake of simplicity we will also neglect the effects of mixing of the S_I , S_R states that can occur if the effective yukawa couplings of the octet carries a phase as discussed in the Appendix. The pair production cross section for the charged scalars is twice that for the real scalars [13] and so is not shown.

⁹Note that setting λ_4 and λ_5 to real values removes the scalar loop contributions to the single production of S_I , which can become large as the values of $\lambda_{4,5}$ increases.

The tree level pair production dominates the loop suppressed single production in the low mass region for small $\lambda_{4,5}$. However as $\lambda_{4,5}$ increase the single production contribution takes over, which occurs at $\lambda_{4,5} \sim 2$ for the neutral scalar, S_R , with a mass of 200 GeV.

A direct search strategy to find octets is to look for narrow resonance structures above the QCD background for states that decay into dijets. CDF has recently performed such a search [45] with 1.13 fb^{-1} of data that could discover octet bound states [41] or single S_i that decay to dijets above the QCD background. The cross sections for the production of these states at the Tevatron, leading to dijet resonance structures, are orders of magnitude below the QCD background in the regions of parameter space we consider, this is shown in Fig. 12

The low mass region is not directly ruled out, although a dedicated study to refine the lower mass bound is warranted due to the shape dependence of the exclusion bound.¹⁰

¹⁰Other possible indirect search strategies for the effects of octet scalars include determining the effect of the octets on the A_{fb}^t . In a similar manner to axiguons [47], these new exotic coloured states could contribute to A_{fb}^t as they are coloured, couple strongly to tops, and are not a vectorlike state. Interestingly, A_{fb}^t has recently been measured [48, 49] to be $A_{FB}^t = 0.19 \pm 0.065(\text{stat}) \pm 0.024(\text{syst})$ which is a deviation larger than 2 sigma from its SM value [47] of $A_{FB}^t = 0.05 \pm 0.015$.

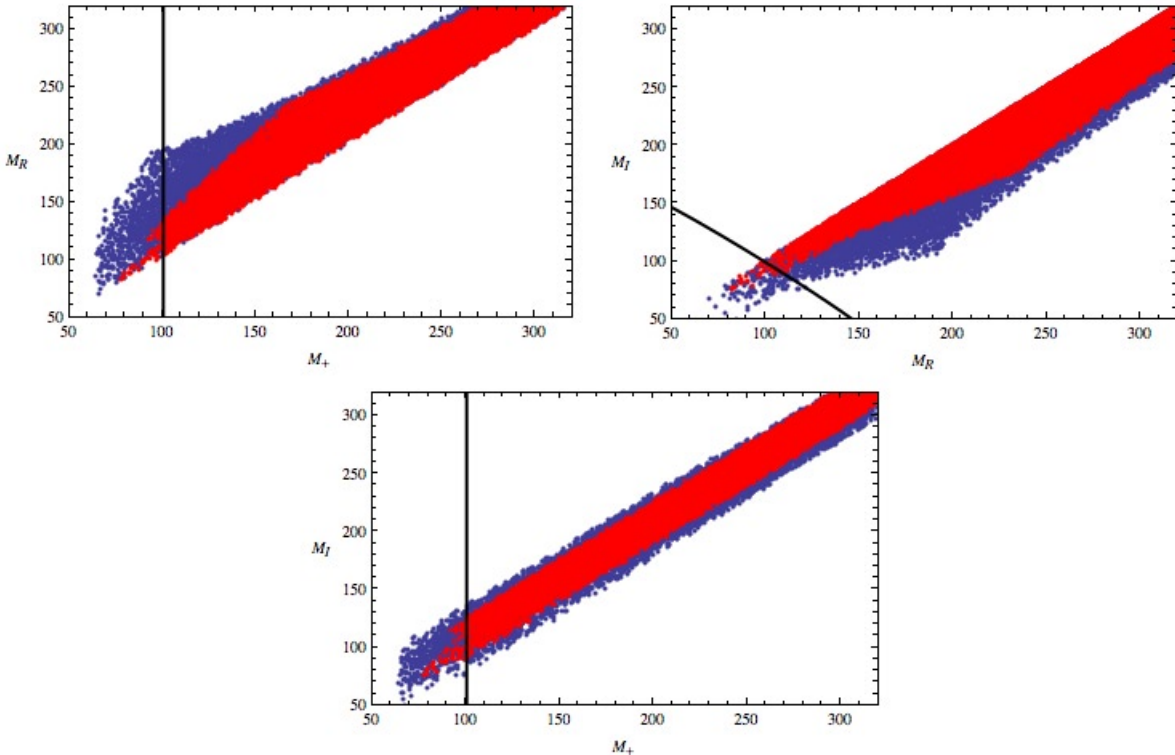


Figure 11: Comparison of the 68% (red or light) and 95% (blue or dark) confidence regions when $\lambda_i < 1$. The LEP2 production bound for ten events is the black line.

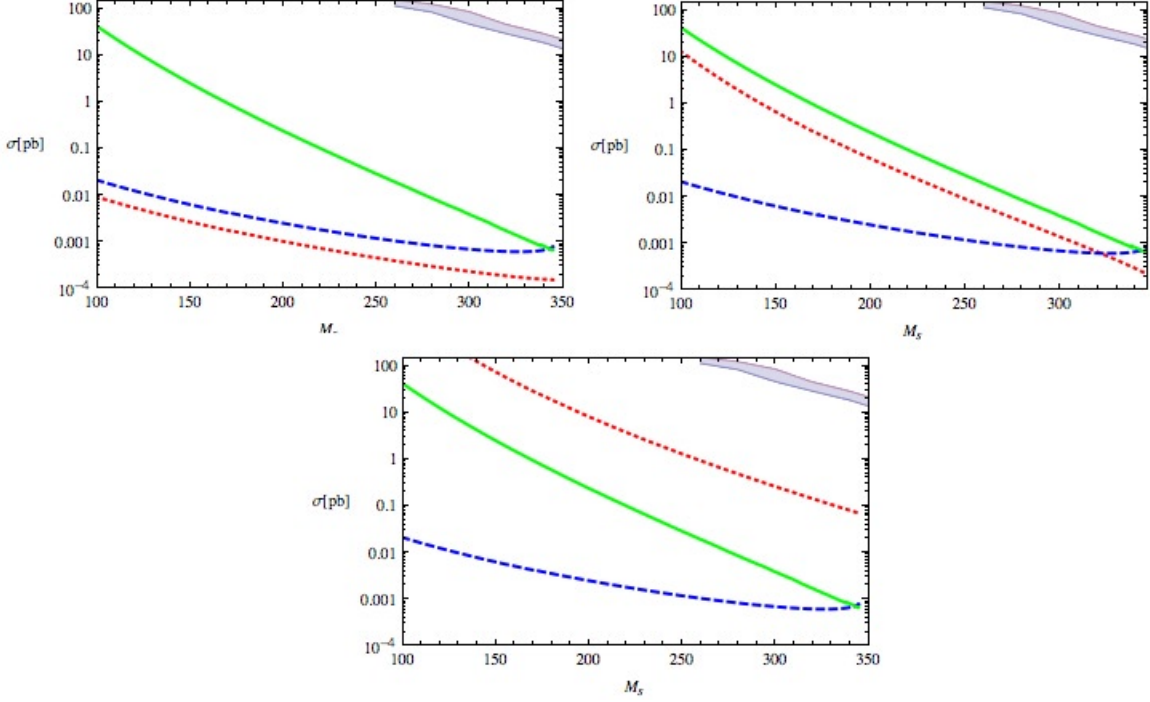


Figure 12: Shown is the production cross section of $\sigma(gg \rightarrow S_R)$ red short dashed line, $\sigma(gg \rightarrow S_I)$ blue long dashed line, and the $\sigma(gg \rightarrow S_R S_R)$ given by the solid green line. The results are for Tevatron with $\sqrt{s} = 1.96$ TeV, $\alpha_s(M_Z) = 0.1217$, $m_t = 173.1$ GeV, $M_Z = 91.1876$ GeV and the NLO CTEQ5 pdfs. The values of (λ_4, λ_5) chosen are $(0, 0)$ upper left, $(1, 1)$ upper right and $(10, 10)$ for the bottom graph. In all three graphs we have set $\eta_U = 0.2$. The dependence on η_U is weak and as η_U decreases the production cross sections decrease. Also shown is a 95% confidence limit band (the shaded region) derived from [45] that places an upper bound on new physics that decays to dijets. The region is defined by the upper limit on $\sigma(X)\mathcal{B}(X \rightarrow jj) * A(|y| < 1)$ where the difference between the W' and RS graviton G^* 95% confidence upper bounds are taken and the acceptance fraction requires the leading jets to have rapidity magnitude $|y| < 1$. The exclusion region depends weakly on the shape of the resonance, so a dedicated study is required to exactly bound the octet decay to dijets, however, the octet signal is orders of magnitude below the exclusion regions obtained from Tevatron before branching and acceptance ratios further reduce the signal. A resummation of large threshold logarithms for single S production was performed in [27]. The K factors for single S production was found to be ~ 2 for 500 GeV a octet mass and this K factor falls as the mass decreases. This indicates that threshold enhancements will not raise the cross section enough to exclude octets for the entire low mass region.

3.3.2 Gauge boson decays and Lepton Signatures

The decays of the octets involving gauge bosons

$$\begin{aligned}
 S_{R,I} &\rightarrow W^\pm S^\mp, & S_{R,I} &\rightarrow Z S_{I,R} \\
 S^\pm &\rightarrow W^\pm S_{R,I}, & S^\pm &\rightarrow Z S^\pm.
 \end{aligned}
 \tag{3.18}$$

were studied in some detail in [13, 28]. These decays are of phenomenological interest as the

gauge bosons can be a source of leptons to trigger on at LHC and Tevatron. The EWPD constraints $|M_{\pm} - M_I| < 50 \text{ GeV}$ and for most of the allowed parameter space $|M_i - M_j| < M_W, M_Z$, as the mass splitting of the doublets scale as v^2/M_s for large masses. This causes the decays to proceed through an offshell gauge boson for most of the allowed parameter space. In this case an effective local operator can be used to approximate the decays.

For example consider $S_R \rightarrow S^- \ell^+ \nu$ through an off shell W . The effective Lagrangian at leading order is given by the product of scalar octet and left handed lepton currents

$$\mathcal{L}_{\text{eff}} = \frac{-i g_1^2}{\sqrt{2} M_W^2} (S_R \partial_{\mu} S_+) (\bar{\nu}_L \gamma^{\mu} \ell_L). \quad (3.19)$$

Exact formula for three body decays such as this exist in the literature [43]. For the masses allowed by EWPD¹¹ generally the energy release is $\Delta = M_R - M_{\pm} < M_R, M_-, M_W$. The resulting decay width at leading order in Δ/M_R is

$$\Gamma_{\ell} = \frac{\alpha^2 \Delta^5}{60 \pi s_W^4 M_W^4}. \quad (3.20)$$

When $M_R > 2 m_t$ the decays to leptons through an offshell W, Z are suppressed decay channels. The dominant decay widths are to $t\bar{b}, t\bar{t}$ unless $\eta_U \ll \eta_D$. The ratio of Γ_{ℓ} to this decay, in the limit $M_R \gg 2 m_t$, is given by

$$\frac{\Gamma_{\ell}}{\Gamma_{S_R^0 \rightarrow t\bar{t}}} \simeq \frac{0.005 \text{ GeV}}{M_R |\eta_U|^2} \left(\frac{\Delta}{50 \text{ GeV}} \right)^5 \quad (3.21)$$

for $\alpha = 1/128$, $s_W = 0.48$ and $m_t = 173 \text{ GeV}$.

When $M_R < 2 m_t$ the offshell W, Z will be dominant decay channels for light masses for much of the parameter space. Taking $m_b = 4.23 \text{ GeV}$, and the other factors as before, the ratio of the offshell decay to the $S_R^0 \rightarrow b\bar{b}$ decay is given by

$$\begin{aligned} \frac{\Gamma_{\ell}}{\Gamma_{S_R^0 \rightarrow b\bar{b}}} &\simeq \frac{4\alpha^2}{15 s_W^4 |\eta_D|^2} \left(\frac{\Delta^5 v^2}{m_W^4 m_b^2 M_R} \right), \\ &\simeq \frac{8 \text{ GeV}}{M_R |\eta_D|^2} \left(\frac{\Delta}{50 \text{ GeV}} \right)^5. \end{aligned} \quad (3.22)$$

If the dominant fermionic decays are to charm quarks due to a mild hierarchy of $\eta_U > (m_b/m_c) \eta_D$, then taking $m_c = 1.3 \text{ GeV}$ gives the branching ratio

$$\frac{\Gamma_{\ell}}{\Gamma_{S_R^0 \rightarrow c\bar{c}}} \simeq \frac{82 \text{ GeV}}{M_R |\eta_U|^2} \left(\frac{\Delta}{50 \text{ GeV}} \right)^5. \quad (3.23)$$

¹¹This assumes that the initial state that is eventually triggered on is not highly boosted. This is generally the case due to the kinematic reach of the Tevatron and LHC.

Thus when quark decays are suppressed through $M_R < 2m_t$ the dominant decay mode will be through an offshell W, Z for much of the parameter space of η_U, η_D allowed by other constraints, notably the constraints due to R_b . This sets a lower bound on the decay width of the heavier octet species given parametrically by Eqn. 3.20. This sets an upper bound on the lifetime of these components of the octet doublet of $4.5/\Delta^5$ ps which yields a upper bound on the decay length of the form $10^{-3}/\Delta^5$ m.¹² Thus the heavier octet species will decay promptly inside the detector and not leave a long lived charged track signature.

As dominant decay modes of the heavy components of the octet doublet (when $M_i < 2m_t$) can be three body decays, the final state signature would be excess monojet or dijet (depending on the boost of the final state octet) events in association with a lepton and missing energy, or enhancements of dilepton signatures with a monojet or dijet. Dedicated studies of these signatures are warranted. The lifetime of the lightest component of the octet doublet is dictated by its decay to fermion pairs.

3.3.3 Constraints from $t\bar{t}$ decays.

For neutral octet masses above $2m_t$, decays into top quark pairs can be dominant. These were previously considered in [40]. The observed limits on excess $\sigma_X \cdot B(X \rightarrow t\bar{t})$ at Tevatron with $0.9 fb^{-1}$ of data [46] do not rule out octets in the intermediate mass region 350 – 1000 GeV. The production cross section for single $gg \rightarrow S_R$ production can become large enough for the bound on $t\bar{t}$ to be relevant, however this requires $\lambda_4 \sim \lambda_5 \sim 75$ which is well into a nonperturbative region of the potential making any conclusion suspect. We illustrate these limits in Fig. 13

3.3.4 Constraints from $\bar{b}b\bar{b}b$ decays.

The dominant decays for light masses will be to quarks $S_+ \rightarrow t\bar{b}$, $S_{R,I} \rightarrow b\bar{b}$ below the $t\bar{t}$ threshold for $\eta_{U,D} \sim \mathcal{O}(1)$. In this regime [28] places a lower bound on the scalar mass of approximately 200 GeV from the CDF search for a scalar particle decaying dominantly to $b\bar{b}$ when produced in association with b quarks [44] This bound is avoided for almost all of the available parameter space for light octet masses. $S_{I,R}$ can decay preferentially to charms, which corresponds to a mild hierarchy of couplings

$$\frac{|\eta_D|^2}{|\eta_U|^2} < \frac{m_c^2}{m_b^2} \sim \frac{1}{10} \quad (3.24)$$

when neglecting $\mathcal{O}(m_{b,c}^2/M_S^2)$ terms. Neutral scalar masses below 200GeV are allowed for $\eta_D \lesssim 0.1$, given an upper limit of $\eta_U \sim 0.3$ from [40] for masses in this range. The three body decays discussed in Section 3.3.2 are actually dominant over quark decays for much of the parameter space allowed by EWPD for light octet masses, invalidating the assumptions of [28] for most of the remaining parameter space.

¹²Here we have converted units assuming that Δ is given in GeV as a pure number, ie for $\Delta = 50$ GeV we have a upper bound on the lifetime of 1.2×10^{-2} as.

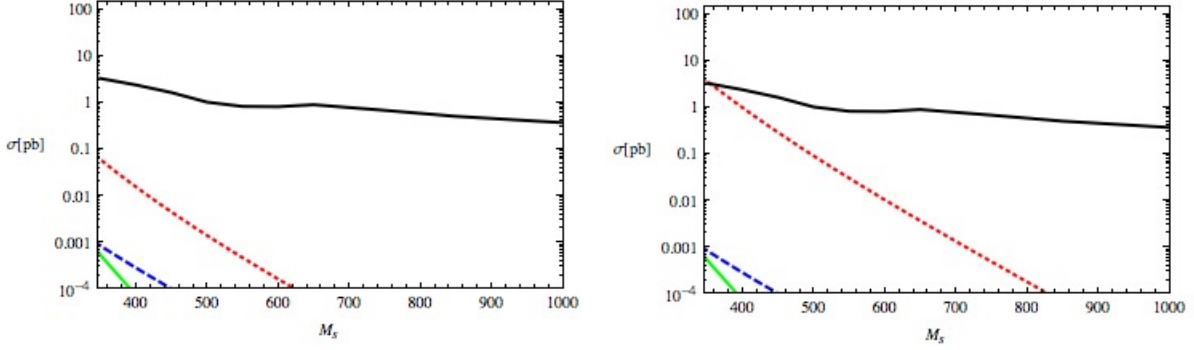


Figure 13: Shown is the production cross section of $\sigma(gg \rightarrow S_R)$ red short dashed line, $\sigma(gg \rightarrow S_I)$ blue long dashed line, and the $\sigma(gg \rightarrow S_R S_R)$ given by the solid green line. The results are for Tevatron with $\sqrt{s} = 1.96$ TeV, $\alpha_s(M_Z) = 0.1217$, $m_t = 173.1$ GeV, $M_Z = 91.1876$ GeV and the NLO CTEQ5 pdfs are used. The D0 95% confidence limit on $\sigma(X)\Gamma(X \rightarrow t\bar{t})$ is the upper solid black line [46]. The values of (λ_4, λ_5) are (10, 10) for the left hand figure and (75, 75) for the right hand figure. $\eta_U = 0.2$ for both figures. For perturbative $\lambda_i \lesssim 10$, current Tevatron production bounds on resonances in $t\bar{t}$ do not rule out octets of mass 350 – 1000 GeV.

3.3.5 Constraints from $\gamma\gamma$ decays.

A promising signature for octets at hadron colliders is the annihilation of a pair of charged octets to photons, $gg \rightarrow S^+ S^- \rightarrow \gamma\gamma$. We can use the recent results of DO [51, 50] that utilize $4.2 fb^{-1}$ of data to place 95% confidence upper limits on $\sigma(h) \times BR(h \rightarrow \gamma\gamma)$ compared to the SM Higgs signal to directly constrain octet annihilation into $\gamma\gamma$. We must consider annihilation decays of octet bound states, octetonia, studied in [41], as the contribution from virtual octets will be a non-resonant signal and the Tevatron Higgs search would not apply. Due to the fact that the results are reported only up to Higgs masses of 150 GeV we are only able to exclude octets up to 75 GeV, which is already disfavoured by LEP2. If the experimental study of $h \rightarrow \gamma\gamma$ is extended to higher Higgs masses at the Tevatron or LHC, this signal is likely to be a significant constraint on the model.

We utilize the fact that this signature has been studied for octetonia in [41] to demonstrate the potential of this signal to raise the mass limit on octets. The ratio we are interested in is that of the octetonia $\sigma(gg \rightarrow O^+) \times BR(O^+ \rightarrow \gamma\gamma)$ to the SM rate for $\sigma(gg \rightarrow h) \times BR(h \rightarrow \gamma\gamma)$. We take [41]

$$\sigma(gg \rightarrow O^+) \times BR(O^+ \rightarrow \gamma\gamma) \approx \frac{9\pi^3 \alpha^2 |\psi(0)|^2}{2M_S \hat{s}^2} \delta(1 - m_O^2/\hat{s}) \quad (3.25)$$

where \hat{s} is the partonic center of mass energy squared and $|\psi(0)|$ is the wavefunction at the origin. We have used the approximation $BR(O^+ \rightarrow \gamma\gamma) \sim \alpha^2/\alpha_s^2(2M_S)$. For the Higgs, we take the approximation

$$\sigma(gg \rightarrow h) \times BR(h \rightarrow \gamma\gamma) \approx \frac{G_F}{\sqrt{2}} \frac{M_H^2 \alpha_s^2}{8\pi \hat{s}} \left(\frac{m_t^4}{M_H^4} \right) 10^{-3} \delta(1 - M_H^2/\hat{s}) \quad (3.26)$$

Neglecting order one factors the ratio of these two signals scales as

$$R \approx 10^6 \frac{\alpha^2}{\alpha_s^2} \frac{|\psi(0)|^2}{\hat{s}} \left(\frac{M_H^2}{M_S m_t^4 G_F} \right) \quad (3.27)$$

This ratio must be less than ~ 35 [51, 50] for $M_h = (100, 150)$ GeV or $M_{\pm} = (50, 75)$ GeV. Unless the wavefunction at the origin was much smaller than its approximate expected value given by [41]

$$|\psi(0)|^2 = \frac{N_c^3 \alpha_s^3 (m_S v) M_S^3}{8 \pi}, \quad (3.28)$$

this bound will likely be violated for this entire mass range. Extending this analysis to higher Higgs masses is expected to raise the lower mass bound on octet states for this reason. For a recent comprehensive study of octetonia signals in gamma gamma for octets from $\sim 200 - 500$ GeV see [41].

3.4 Flavour constraints reexamined for light scalars

Flavour constraints on $(\mathbf{8}, \mathbf{2})_{1/2}$ scalars were examined in some detail in linear MFV¹³ in [13] when the masses of the octet scalars were considered to be \sim TeV. However, although MFV suppresses flavour changing effects and ensures the vanishing of tree level flavour changing neutral currents in linear MFV, when one goes beyond leading order in the Yukawa couplings problematic flavour changing neutral currents are possible [40]. The correct way to examine such flavour issues is to utilize a nonlinear representation of MFV¹⁴ such as formulated in [10, 11, 12] which is beyond the scope of this work.

We have reexamined the flavour constraints that were examined in [13] in linear MFV for the light octet masses allowed by EWPD and not ruled out by direct production bounds. Flavour constraints are largely irrelevant for $|\eta_U|$ once the far more restrictive constraint from R_b is known. To quantitatively demonstrate this consider $K^0 - \bar{K}^0$ mixing for relatively light masses $M_s = 300 (400)$ GeV. We use the results of [13] for the contribution of the octets to the wilson coefficient (C_s) of the operator $(V_{td}^* V_{ts})(d_L \gamma^\nu s_L)(d_L \gamma^\nu s_L)$ and use the SM expression of [52] for the contribution of this operator to $K^0 - \bar{K}^0$ mixing and hence $|\epsilon_K|$. One finds that the contribution of the octets to $|\epsilon_K|$ is given by

$$\Delta|\epsilon_K| = |C_\epsilon B_K \text{Im}[V_{td}^* V_{ts}] \text{Re}[V_{td}^* V_{ts}] C_S| \quad (3.29)$$

Using the measured values $m_K = 497.6$ MeV, $f_K = (156.1 \pm 0.8)$ MeV, $(\Delta M_K)_{exp} = 3.483 \pm 0.006) \times 10^{-12}$ MeV one obtains

$$C_\epsilon = \frac{G_F^2 F_K^2 m_K M_W^2}{6 \sqrt{2} \pi^2 \Delta M_K} = 3.65 \times 10^4. \quad (3.30)$$

¹³Where one only utilizes a linear yukawa coupling for the scalars.

¹⁴We thanks J. Zupan for discussions on this point.

Further, Lattice QCD [53] gives the input $B_K(2 \text{ GeV}) = 0.54 \pm 0.05$, and using the central values of fitted values for the CKM parameters $A, \bar{\eta}, \bar{\rho}, \lambda$ from the PDG we find that the shift in $|\epsilon_K|$ is given by

$$\Delta|\epsilon_K| = 1.5 (1.6) \times 10^{-12} (|\eta_U|^2 + 6 (3) |\eta_U|^4) \quad (3.31)$$

for $M_s = 300 (400) \text{ GeV}$. Considering $|\epsilon_K|_{exp} = (2.229 \pm 0.010) \times 10^{-3}$ while the same values employed above gives the central value $|\epsilon_K|_{theory} = 1.70 \times 10^{-3}$ one can set an upper limit on $|\eta_U|$ from $K^0 - \bar{K}^0$ mixing by conservatively assigning one tenth of the discrepancy between theory and experiment to the effect of octets. This gives an upper bound on $|\eta_U|$ of 48 (56) for $M_s = 300 (400) \text{ GeV}$. The weak mass dependence of the bound allows one to neglect Kaon mixing constraints for low masses, compared to R_b constraints on $|\eta_U|$, for light masses $M_s \ll 1 \text{ TeV}$, in linear MFV.

The $B \rightarrow X_s \gamma$ decay rate constrains the combination $|\eta_U \eta_D|$, in the limit η_U is small, and was calculated in [13]. Using their result and the upper bound on $|\eta_U|$ from R_b , we determine the strongest upper bound on $|\eta_D|$ for light masses by requiring that the octet contribution to $B \rightarrow X_s \gamma$ is less than the $\sim 10\%$ SM theoretical and experimental errors. For $M_\pm = (75, 100, 200)$ and the corresponding maximum $|\eta_U| = (0.26, 0.27, 0.33)$, one obtains an upper bound on $|\eta_D|$ of $(0.36, 0.39, 0.50)$. As $|\eta_U|$ decreases, the upper bound on $|\eta_D|$ is relaxed.

Finally, the electric dipole moment of the neutron constrains the imaginary part of the η_i and using [13] we find for light masses that $\text{Im}[\eta_U^* \eta_D^*] < 1/10$ for $m_S = 100 \text{ GeV}$.

4. Conclusions

We have considered the phenomenological constraints of the general scalar sector that contains one $(\mathbf{1}, \mathbf{2})_{1/2}$ Higgs doublet and a one $(\mathbf{8}, \mathbf{2})_{1/2}$ colour octet scalar doublet. To this end we have performed a modern fit in the STU and STUVWX approaches to EWPD and used these results to determine the allowed masses for light octets. We have demonstrated that, somewhat surprisingly, the six parameter fit formalism is more restrictive for light states due to strong correlations amongst the fit observables. We find that the octet doublet masses can be in the 100 GeV range. Such light octets can significantly effect the discovery strategies for a light Higgs by modifying the Higgs production mechanism through a one loop contribution to $gg \rightarrow h$ that is not well approximated by a local operator. Octets will also induce a further effective coupling at one loop between h and $\gamma\gamma$, ZZ and W^+W^- and would significantly effect Higgs discovery at LHC [54]. Despite this, we have shown that current production bounds on light octets at LEP2 and Tevatron do not rule out the low mass region and further studies for narrow resonances in the dijet invariant mass distribution and $h \rightarrow \gamma\gamma$ signal are required. Currently, octets are another example of physics beyond the SM that can significantly effect the properties of the Higgs and yet are otherwise relatively unconstrained

experimentally.¹⁵ For light octets, one possible alternate search strategy is to utilize the Higgs p_T distribution [57] to find indirect evidence for onshell octet scalars that have eluded direct detection.

We have also performed a joint fit for the Higgs and the octets by varying the Higgs mass oblique corrections at one loop while allowing the masses of the octets to vary. Doing so we have demonstrated a mechanism that is quite general in its effect of giving a positive contribution to the T parameter when an extra doublet is present and fit to in EWPD. This allows the Higgs and octet to be simultaneously heavy and the Higgs can be as massive as its unitarity bound. For the parameter space where the Higgs mass is raised, h decaying to pairs of octets is kinematically suppressed. The search strategy for the heavy Higgs remains substantially the same with difficulties in constructing a mass peak due to the width of the Higgs resonance and large irreducible backgrounds to SM processes producing $W^+ W^-$ decays such as from $\bar{t}t$, and large Wj backgrounds. Likewise very heavy octets are also very broad resonances for large masses and are difficult to discover at hadron colliders with decays to $\bar{t}t$ dominating, and large SM backgrounds. Further dedicated studies of LHC phenomenology of this scenario are warranted, as are further dedicated studies to attempt to raise the lower mass bounds on octet scalar doublets.

Acknowledgements

We sincerely thank B Batell for extensive collaboration during this work.

We also thank Mark Wise, Maxim Pospelov and Aneesh Manohar for comments on the manuscript. We thank Michael Luke for many helpful discussions and Jens Erler for communication on the EWPD fits. We are particularly grateful to Aneesh Manohar for an extensive debate on the precise nature of the new $SU(2)_C$ constraint on the potential, which he won.

This work was partially supported by funds from the Natural Sciences and Engineering Research Council (NSERC) of Canada. Research at the Perimeter Institute is supported in part by the Government of Canada through NSERC and by the Province of Ontario through MRI.

¹⁵For further studies of the modification of the properties of the Higgs through otherwise experimentally elusive new physics see [55, 56].

A. EWPD fit

The data and theory predictions used in constructing the fit are given in Table 2.

Observable	Data Used	Theory Prediction
M_W [GeV]	80.428 ± 0.039	80.380 ± 0.015
	80.376 ± 0.033	80.380 ± 0.015
M_Z [GeV]	91.1876 ± 0.0021	91.1874 ± 0.0021
Γ_Z [GeV]	2.4952 ± 0.0023	2.4954 ± 0.0009
Γ_{had} [GeV]	1.7444 ± 0.0020	1.7419 ± 0.0009
Γ_{inv} [MeV]	499.0 ± 1.5	501.68 ± 0.07
Γ_{l+l^-} [MeV]	83.984 ± 0.086	84.002 ± 0.016
σ_{had} [nb]	41.541 ± 0.037	41.483 ± 0.008
R_e	20.804 ± 0.050	20.736 ± 0.010
R_μ	20.785 ± 0.033	20.736 ± 0.010
R_τ	20.764 ± 0.045	20.736 ± 0.010
R_b	0.21629 ± 0.00066	0.21578 ± 0.00005
R_c	0.1721 ± 0.0030	0.17224 ± 0.00003
A_{FB}^e	0.0145 ± 0.0025	0.01627 ± 0.00023
A_{FB}^μ	0.0169 ± 0.0013	0.01627 ± 0.00023
A_{FB}^τ	0.0188 ± 0.0017	0.01627 ± 0.00023
A_{FB}^b	0.0992 ± 0.0016	0.1033 ± 0.0007
A_{FB}^c	0.0707 ± 0.0035	0.0738 ± 0.0006
$\bar{s}_l^2(A_{FB}^q)$	0.2316 ± 0.0018	0.2315 ± 0.0001
A_e	0.15138 ± 0.00216	0.1473 ± 0.0010
	0.1544 ± 0.0060	0.1473 ± 0.0010
	0.1498 ± 0.0049	0.1473 ± 0.0010
A_μ	0.142 ± 0.015	0.1473 ± 0.0010
A_τ	0.136 ± 0.015	0.1473 ± 0.0010
	0.1439 ± 0.0043	0.1473 ± 0.0010
A_b	0.923 ± 0.020	0.9347 ± 0.0001
A_c	0.670 ± 0.027	0.6679 ± 0.0004
g_L^2	0.3010 ± 0.0015	0.3039 ± 0.0002
g_R^2	0.0308 ± 0.0011	0.03000 ± 0.00003
$g_V^{\nu e}$	-0.040 ± 0.015	-0.0397 ± 0.0003
$g_A^{\nu e}$	-0.507 ± 0.014	-0.5064 ± 0.0001
$Qw(Cs)$	-73.16 ± 0.35	-73.16 ± 0.03
$Qw(Tl)$	-116.4 ± 3.6	-116.8 ± 0.04
Γ_W [GeV]	2.141 ± 0.041	2.0902 ± 0.0009

Table 2: Observables used in fit to oblique parameters.

The numbers we use for the theory predictions are based on the 2008 PDG results of a global fit to the EWPD. The input values used in the theory predictions are

$$\begin{aligned}
M_Z &= 91.1876 \pm 0.0021 \text{ GeV}, & M_H &= 96_{-24}^{+29} \text{ GeV}, \\
m_t &= 173.1 \pm 1.4 \text{ GeV}, & \alpha_s(M_Z) &= 0.1217 \pm 0.0017 \text{ GeV}, \\
\hat{\alpha}(M_Z)^{-1} &= 127.909 \pm 0.0019, & \Delta \alpha_{had}^{(5)} &\approx 0.02799 \pm 0.00014.
\end{aligned} \tag{A.1}$$

The definitions of the oblique corrections we use are

$$\begin{aligned}
\frac{\alpha S}{4s_W^2 c_W^2} &= \left[\frac{\delta\Pi_{ZZ}(M_Z^2) - \delta\Pi_{ZZ}(0)}{M_Z^2} \right] - \frac{(c_W^2 - s_W^2)}{s_W c_W} \delta\Pi'_{Z\gamma}(0) - \delta\Pi'_{\gamma\gamma}(0), \\
\alpha T &= \frac{\delta\Pi_{WW}(0)}{M_W^2} - \frac{\delta\Pi_{ZZ}(0)}{M_Z^2}, \\
\frac{\alpha U}{4s_W^2} &= \left[\frac{\delta\Pi_{WW}(M_W^2) - \delta\Pi_{WW}(0)}{M_W^2} \right] - c_W^2 \left[\frac{\delta\Pi_{ZZ}(M_Z^2) - \delta\Pi_{ZZ}(0)}{M_Z^2} \right] \\
&\quad - s_W^2 \delta\Pi'_{\gamma\gamma}(0) - 2 s_W c_W \delta\Pi'_{Z\gamma}(0), \\
\alpha V &= \delta\Pi'_{ZZ}(M_Z^2) - \left[\frac{\delta\Pi_{ZZ}(M_Z^2) - \delta\Pi_{ZZ}(0)}{M_Z^2} \right], \\
\alpha W &= \delta\Pi'_{WW}(M_W^2) - \left[\frac{\delta\Pi_{WW}(M_W^2) - \delta\Pi_{WW}(0)}{M_W^2} \right], \\
\alpha X &= -s_W c_W \left[\frac{\delta\Pi_{Z\gamma}(M_Z^2)}{M_Z^2} - \delta\Pi'_{Z\gamma}(0) \right]
\end{aligned} \tag{A.2}$$

The self energies to determine these results are given by the following in terms of PV functions that match the definitions in [42] and are

$$\begin{aligned}
16 \pi^2 \mu^{4-n} \int \frac{d^n q}{i (2\pi)^n} \frac{1}{q^2 - m^2 + i\epsilon} &= A_0(m^2) \\
16 \pi^2 \mu^{4-n} \int \frac{d^n q}{i (2\pi)^n} \frac{1}{[q^2 - m_1^2 + i\epsilon] [(q-p)^2 - m_2^2 + i\epsilon]} &= B_0(p^2, m_1^2, m_2^2) \\
16 \pi^2 \mu^{4-n} \int \frac{d^n q}{i (2\pi)^n} \frac{q_\mu}{[q^2 - m_1^2 + i\epsilon] [(q-p)^2 - m_2^2 + i\epsilon]} &= p_\mu B_1(p^2, m_1^2, m_2^2) \\
16 \pi^2 \mu^{4-n} \int \frac{d^n q}{i (2\pi)^n} \frac{q_\mu q_\nu}{[q^2 - m_1^2 + i\epsilon] [(q-p)^2 - m_2^2 + i\epsilon]} &= p_\mu p_\nu B_{21}(p^2, m_1^2, m_2^2), \\
&\quad + g_{\mu\nu} B_{22}(p^2, m_1^2, m_2^2)
\end{aligned} \tag{A.3}$$

Our results are

$$\begin{aligned}
\delta\Pi_{WW}(p^2) &= \frac{g_1^2}{2\pi^2} \left[B_{22}(p^2, M_I^2, M_+^2) + B_{22}(p^2, M_R^2, M_+^2) \right. \\
&\quad \left. - \frac{1}{2} A_0(M_+^2) - \frac{1}{4} A_0(M_R^2) - \frac{1}{4} A_0(M_I^2) \right]
\end{aligned} \tag{A.4}$$

$$\begin{aligned} \delta\Pi_{ZZ}(p^2) &= \frac{g_1^2}{2\pi^2 c_W^2} \left[(1 - 2s_W^2)^2 \left(B_{22}(p^2, M_+^2, M_+^2) - \frac{1}{2}A_0(M_+^2) \right) \right. \\ &\quad \left. + B_{22}(p^2, M_R^2, M_I^2) - \frac{1}{4}A_0(M_R^2) - \frac{1}{4}A_0(M_I^2) \right] \end{aligned} \quad (\text{A.5})$$

$$\delta\Pi_{\gamma\gamma}(p^2) = \frac{2e^2}{\pi^2} \left[B_{22}(p^2, M_+^2, M_+^2) - \frac{1}{2}A_0(M_+^2) \right] \quad (\text{A.6})$$

$$\delta\Pi_{\gamma Z}(p^2) = \frac{eg_1(1 - 2s_W^2)}{\pi^2 c_W} \left[B_{22}(p^2, M_+^2, M_+^2) - \frac{1}{2}A_0(M_+^2) \right] \quad (\text{A.7})$$

For $p^2 = 0$ these expressions become

$$\delta\Pi_{WW}(0) = \frac{g_1^2}{8\pi^2} \left(\frac{1}{2}f(M_+, M_R) + \frac{1}{2}f(M_+, M_I) \right) \quad (\text{A.8})$$

$$\delta\Pi_{ZZ}(0) = \frac{g_1^2}{8\pi^2 c_W^2} \left(\frac{1}{2}f(M_R, M_I) \right) \quad (\text{A.9})$$

where

$$f(m_1, m_2) = m_1^2 + m_2^2 - \frac{2m_1^2 m_2^2}{m_1^2 - m_2^2} \log \frac{m_1^2}{m_2^2} \quad (\text{A.10})$$

The derivatives of the vacuum polarizations are

$$\delta\Pi'_{\gamma\gamma}(0) = -\frac{e^2}{6\pi^2} B_0(0, M_+^2, M_+^2) \quad (\text{A.11})$$

$$\delta\Pi'_{\gamma Z}(0) = -\frac{eg_1(1 - 2s_W^2)}{12\pi^2 c_W} B_0(0, M_+^2, M_+^2) \quad (\text{A.12})$$

B. Renormalization

We use dim reg in $d = 4 - 2\epsilon$ dimensions. We introduce wavefunction renormalization and mass renormalization constants for the octet fields as usual

$$S_i = \frac{S_i^{(0)}}{\sqrt{Z_i}}, \quad M_i = \frac{M_i^{(0)}}{\sqrt{Z_{Mi}}}. \quad (\text{B.1})$$

However, in choosing renormalization conditions, we note that to define the masses and the mass splittings one cannot use $\overline{\text{MS}}$, as in $\overline{\text{MS}}$ the mass is defined to have only the divergence subtracted from the bare mass. The resulting renormalized mass in $\overline{\text{MS}}$ is not shifted by the finite components of the loop corrections that we have determined. The renormalization prescription we use is the zero-momentum subtraction scheme [58], where we require that the self energy and its derivative with respect to external momentum, p^2 , vanishes at $p^2 \rightarrow 0$. Note that the second derivative term in the Taylor expansion of the self energy does not contribute until two loop order and therefore can be neglected here. The counter terms in the lagrangian are given by

$$\sum_i [(Z_i - 1)(\partial^\mu S_i \partial_\mu S_i) - (Z_i Z_{Mi} - 1)M_i^2 S_i^2]. \quad (\text{B.2})$$

With this prescription the wavefunction renormalization and the mass counterterm are of the form

$$\begin{aligned} Z_i &= 1 - \frac{a}{\epsilon} - \frac{d \Sigma_i(p^2)}{d p^2} \Big|_{p^2 \rightarrow 0} \\ Z_{Mi} &= 1 + \frac{b}{\epsilon} + \Sigma_i(p^2) \Big|_{p^2 \rightarrow 0} + (1 - Z_i) \end{aligned} \quad (\text{B.3})$$

where a, b are the coefficients of the p^2, M^2 dependent one loop divergences respectively and the Σ_i are the finite terms of the one loop self energy.

Using this scheme and the divergence properties of the PV functions, the wavefunction renormalization factors are determined to be

$$\begin{aligned} Z_I &= 1 - \frac{y_t^2 |\eta_U|^2 + y_b^2 |\eta_D|^2}{64 \pi^2 \epsilon} + \frac{g_1^2}{32 \pi^2 \epsilon} \left[1 + \frac{1}{2 c_W^2} \right] + \frac{y_t^2 |\eta_U|^2 \log \left[\frac{m_t^2}{\mu^2} \right] + y_b^2 |\eta_D|^2 \log \left[\frac{m_b^2}{\mu^2} \right]}{32 \pi^2} \\ &\quad + \frac{y_t^2 \text{Im}[\eta_U]^2 + y_b^2 \text{Im}[\eta_D]^2}{48 \pi^2} + \frac{g_1^2}{16 \pi^2} \left[b_0(0, M_W^2, m_\pm^2) + \frac{b_0(0, M_Z^2, M_R^2)}{2 c_W^2} \right] \\ Z_R &= 1 - \frac{y_t^2 |\eta_U|^2 + y_b^2 |\eta_D|^2}{64 \pi^2 \epsilon} + \frac{g_1^2}{32 \pi^2 \epsilon} \left[1 + \frac{1}{2 c_W^2} \right] + \frac{y_t^2 |\eta_U|^2 \log \left[\frac{m_t^2}{\mu^2} \right] + y_b^2 |\eta_D|^2 \log \left[\frac{m_b^2}{\mu^2} \right]}{32 \pi^2} \\ &\quad + \frac{y_t^2 \text{Re}[\eta_U]^2 + y_b^2 \text{Re}[\eta_D]^2}{48 \pi^2} + \frac{g_1^2}{16 \pi^2} \left[b_0(0, M_W^2, M_\pm^2) + \frac{b_0(0, M_Z^2, M_I^2)}{2 c_W^2} \right] \\ Z_\pm &= 1 - \frac{y_t^2 |\eta_U|^2 + y_b^2 |\eta_D|^2}{64 \pi^2 \epsilon} + \frac{g_1^2}{32 \pi^2 \epsilon} \left[1 + \frac{(1 - 2 s_W^2)^2}{2 c_W^2} + 2 s_W^2 \right] \\ &\quad + \frac{g_1^2}{32 \pi^2} \left[b_0(0, M_W^2, M_I^2) + b_0(0, M_W^2, M_R^2) + \frac{(1 - 2 s_W^2)^2 b_0(0, M_Z^2, M_\pm^2)}{c_W^2} - 4 s_W^2 \left(\log \left[\frac{M_\pm^2}{\mu^2} \right] - 1 \right) \right] \\ &\quad - \frac{(y_b^2 |\eta_D|^2 + y_t^2 |\eta_U|^2)}{32 \pi^2} b_0(0, m_b^2, m_t^2) \end{aligned} \quad (\text{B.4})$$

Using these results the mass renormalization factors are determined to be

$$\begin{aligned} Z_{MI} &= (2 - Z_I) - \frac{v^2}{32 \pi^2 M_I^2} \left[y_t^4 (\text{Re}[\eta_U]^2 + 3 \text{Im}[\eta_U]^2) \left(\frac{1}{2 \epsilon} - \log \left[\frac{m_t^2}{\mu^2} \right] \right) \right. \\ &\quad \left. + y_b^4 (\text{Re}[\eta_D]^2 + 3 \text{Im}[\eta_D]^2) \left(\frac{1}{2 \epsilon} - \log \left[\frac{m_b^2}{\mu^2} \right] \right) \right] - \frac{v^2 (y_t^4 |\eta_U|^2 + y_b^4 |\eta_D|^2)}{32 \pi^2 M_I^2} \\ &\quad + \frac{g_1^2}{64 \pi^2 M_I^2 \epsilon} \left[3 M_W^2 - M_\pm^2 + \frac{(3 M_Z^2 - M_R^2)}{2 c^2} \right] \\ &\quad + \frac{g_1^2}{32 \pi^2 M_I^2} \left[(M_W^2 - 2 M_\pm^2) b_0[0, M_W, M_\pm] + \frac{(M_Z^2 - 2 M_R^2) b_0[0, M_Z, M_R]}{2 c_W^2} \right] \\ &\quad + M_\pm^2 \left(1 - \log \left[\frac{M_\pm^2}{\mu^2} \right] \right) + M_W^2 \left(1 - 2 \log \left[\frac{M_W^2}{\mu^2} \right] \right) + \frac{M_Z^2}{2 c_W^2} \left(1 - 2 \log \left[\frac{M_Z^2}{\mu^2} \right] \right) \\ &\quad + \frac{M_R^2}{2 c_W^2} \left(1 - \log \left[\frac{M_R^2}{\mu^2} \right] \right) \end{aligned} \quad (\text{B.5})$$

$$\begin{aligned}
Z_{MR} &= Z_{MI} \Big|_{M_R^2 \rightarrow M_I^2, Z_I \rightarrow Z_R, \text{Re} \leftrightarrow \text{Im}} \\
Z_{M\pm} &= (2 - Z_{\pm}) - \frac{v^2 y_b^4 |\eta_D|^2}{64 \pi^2 M_{\pm}^2} \left[\frac{1}{\epsilon} + b_0[0, m_b, m_t] - \log \left[\frac{m_b^2}{\mu^2} \right] + 1 \right] \\
&\quad - \frac{v^2 y_t^4 |\eta_U|^2}{64 \pi^2 M_{\pm}^2} \left[\frac{1}{\epsilon} + b_0[0, m_b, m_t] - \log \left[\frac{m_t^2}{\mu^2} \right] + 1 \right] \\
&\quad - \frac{y_b^2 y_t^2 v^2}{64 \pi^2 M_{\pm}^2} \left[|\eta_D|^2 \left(\frac{1}{\epsilon} - \log \left[\frac{m_t^2}{\mu^2} \right] + 1 + b_0[0, m_b, m_t] \right) \right. \\
&\quad \left. + |\eta_U|^2 \left(\frac{1}{\epsilon} - \log \left[\frac{m_b^2}{\mu^2} \right] + 1 + b_0[0, m_b, m_t] \right) - (\eta_D \eta_U + \eta_D^* \eta_U^*) \left(\frac{1}{\epsilon} + 2 b_0[0, m_b, m_t] \right) \right] \\
&\quad + \frac{g_1^2}{32 \pi^2 \epsilon} \left[\frac{6 M_W^2 - M_R^2 - M_I^2}{4 M_{\pm}^2} + \frac{(1 - 2s_W^2)^2 (3 M_Z^2 - M_{\pm}^2)}{4 c_W^2 M_{\pm}^2} - s_W^2 \right] \\
&\quad + \frac{g_1^2}{64 \pi^2 M_{\pm}^2} \left[(M_W^2 - 2 M_I^2) b_0[0, M_W, M_I] + (M_W^2 - 2 M_R^2) b_0[0, M_W, M_R] \right. \\
&\quad \left. + (M_Z^2 - 2 M_{\pm}^2) \frac{(1 - 2s_W^2)^2}{c_W^2} b_0[0, M_Z, M_{\pm}] + M_I^2 \left(1 - \log \left[\frac{M_I^2}{\mu^2} \right] \right) \right. \\
&\quad \left. + M_R^2 \left(1 - \log \left[\frac{M_R^2}{\mu^2} \right] \right) + 2 M_W^2 \left(1 - 2 \log \left[\frac{M_W^2}{\mu^2} \right] \right) \right. \\
&\quad \left. + \frac{M_Z^2 (1 - 2s_W^2)^2}{c_W^2} \left(1 - 2 \log \left[\frac{M_Z^2}{\mu^2} \right] \right) + M_{\pm}^2 \frac{8s_W^4 - 8s_W^2 + 1}{c_W^2} \left(1 - \log \left[\frac{M_{\pm}^2}{\mu^2} \right] \right) \right] \quad (\text{B.6})
\end{aligned}$$

The remaining renormalization is for the mixing operator $S_R S_I$ which is renormalized as usual by introducing a further counter term to subtract the only divergences of composite operators as in $\overline{\text{MS}}$

$$\frac{\sqrt{Z_I} \sqrt{Z_R} (v^2 S_R S_I)}{Z_{RI}} \quad (\text{B.7})$$

where

$$Z_{RI} = 1 + \frac{Z_R - 1}{2} + \frac{Z_I - 1}{2} + \frac{y_t^4 \text{Re}[\eta_U] \text{Im}[\eta_U] - y_b^4 \text{Re}[\eta_D] \text{Im}[\eta_D]}{32 \pi^2 \epsilon} \quad (\text{B.8})$$

C. Mixing of S_R and S_I

For completeness in examining one loop effects we determine the mixing between S_R and S_I . The mass matrix is given by

$$M_{RI} = \begin{pmatrix} M_I^2 + \delta \langle T \{ S^I S^I \} \rangle_G + \delta \langle T \{ S^I S^I \} \rangle_Y & \delta \langle T \{ S^R S^I \} \rangle_Y \\ \delta \langle T \{ S^R S^I \} \rangle_Y & M_R^2 + \delta \langle T \{ S^R S^R \} \rangle_G + \delta \langle T \{ S^R S^R \} \rangle_Y \end{pmatrix}. \quad (\text{C.1})$$

We diagonalize the mass matrix by introducing a mixing angle and rotating the S_R, S_I fields to a diagonal mass basis S'_R, S'_I via

$$\begin{pmatrix} S_I \\ S_R \end{pmatrix} = \begin{pmatrix} \cos(\theta) & \sin(\theta) \\ -\sin(\theta) & \cos(\theta) \end{pmatrix} \begin{pmatrix} S'_I \\ S'_R \end{pmatrix}. \quad (\text{C.2})$$

The mixing angle is given by

$$\sin(\theta) = \frac{|y_t^4 B_0^*(p^2, m_t^2, m_t^2) \text{Re}(\eta_U) \text{Im}(\eta_U) - y_b^4 B_0^*(p^2, m_b^2, m_b^2) \text{Re}(\eta_D) \text{Im}(\eta_D)|}{8 \pi^2 \lambda_2} \quad (\text{C.3})$$

where B_0^* is the usual PV function with the divergence subtracted given by

$$B_0^*(p^2, m_i^2, m_i^2) = -2 + \log\left(\frac{m_i^2}{\mu^2}\right) - \beta \log\left(\frac{1 + \beta}{1 - \beta}\right) \quad (\text{C.4})$$

where $\beta = \sqrt{1 - 4m_i^2/p^2}$, which would be the velocity of the scalar produced in the CM frame which was subsequently to mix into another state with mass m_j . We take $p^2 = m_s^2$ as the mass splittings are a small perturbation in a radiatively induced mixing. If we take $\mu \simeq 1 \text{ TeV}$ as the scale at which we impose exact $\text{SU}(2_C)$ on our scalar potential, this gives a mixing angle

$$\sin(\theta) \simeq 0.04 \frac{|\text{Re}(\eta_U)| |\text{Im}(\eta_U)|}{\lambda_2}, \quad (\text{C.5})$$

which depends weakly on the value of m_s as the numerical coefficient changes by 25% for m_s varying between 0.01 – 300 GeV. This mixing angle, if non zero, will effect the production cross section of the S_I, S_R states at LHC and Tevatron, and introduce mixing between the octetonia states discussed in [41].

References

- [1] L. Susskind, “Dynamics Of Spontaneous Symmetry Breaking In The Weinberg-Salam Theory,” *Phys. Rev. D* **20** (1979) 2619.
- [2] S. Weinberg, “Implications Of Dynamical Symmetry Breaking: An Addendum,” *Phys. Rev. D* **19** (1979) 1277.
- [3] P. Sikivie, L. Susskind, M. B. Voloshin and V. I. Zakharov, “Isospin Breaking In Technicolor Models,” *Nucl. Phys. B* **173** (1980) 189.
- [4] R. S. Chivukula and H. Georgi, “Composite Technicolor Standard Model,” *Phys. Lett. B* **188** (1987) 99.
- [5] L. J. Hall and L. Randall, “Weak scale effective supersymmetry,” *Phys. Rev. Lett.* **65**, 2939 (1990).
- [6] G. D’Ambrosio, G. F. Giudice, G. Isidori and A. Strumia, “Minimal flavour violation: An effective field theory approach,” *Nucl. Phys. B* **645** (2002) 155 [arXiv:hep-ph/0207036].

- [7] V. Cirigliano, B. Grinstein, G. Isidori and M. B. Wise, “Minimal flavor violation in the lepton sector,” Nucl. Phys. B **728** (2005) 121 [arXiv:hep-ph/0507001].
- [8] A. J. Buras, “Minimal flavor violation,” Acta Phys. Polon. B **34** (2003) 5615 [arXiv:hep-ph/0310208].
- [9] G. C. Branco, A. J. Buras, S. Jager, S. Uhlig and A. Weiler, “Another look at minimal lepton flavour violation, $l(i) \rightarrow l(j) \gamma$, leptogenesis, and the ratio $M(\nu)/\Lambda(\text{LFV})$,” JHEP **0709** (2007) 004 [arXiv:hep-ph/0609067].
- [10] T. Feldmann and T. Mannel, “Large Top Mass and Non-Linear Representation of Flavour Symmetry,” Phys. Rev. Lett. **100** (2008) 171601 [arXiv:0801.1802 [hep-ph]].
- [11] A. L. Kagan, G. Perez, T. Volansky and J. Zupan, “General Minimal Flavor Violation,” arXiv:0903.1794 [hep-ph].
- [12] T. Feldmann, M. Jung and T. Mannel, “Sequential Flavour Symmetry Breaking,” arXiv:0906.1523 [hep-ph].
- [13] A. V. Manohar and M. B. Wise, “Flavor changing neutral currents, an extended scalar sector, and the Higgs production rate at the LHC,” Phys. Rev. D **74** (2006) 035009 [arXiv:hep-ph/0606172].
- [14] J. Erler, P. Langacker, S. Munir and E. R. Pena, “Improved Constraints on Z' Bosons from Electroweak Precision Data,” arXiv:0906.2435 [hep-ph].
- [15] R. Barbieri and A. Strumia, arXiv:hep-ph/0007265.
- [16] T. Plehn and T. M. P. Tait, “Seeking Sgluons,” J. Phys. G **36**, 075001 (2009) [arXiv:0810.3919 [hep-ph]].
- [17] S. Y. Choi, M. Drees, J. Kalinowski, J. M. Kim, E. Popeno and P. M. Zerwas, “Color-Octet Scalars of $N=2$ Supersymmetry at the LHC,” Phys. Lett. B **672**, 246 (2009) [arXiv:0812.3586 [hep-ph]].
- [18] C. T. Hill, “Topcolor: Top Quark Condensation In A Gauge Extension Of The Standard Model,” Phys. Lett. B **266** (1991) 419.
- [19] B. A. Dobrescu, K. Kong and R. Mahbubani, Phys. Lett. B **670**, 119 (2008) [arXiv:0709.2378 [hep-ph]].
- [20] B. A. Dobrescu, K. Kong and R. Mahbubani, JHEP **0707**, 006 (2007) [arXiv:hep-ph/0703231].
- [21] P. Y. Popov, A. V. Povarov and A. D. Smirnov, “Fermionic decays of scalar leptoquarks and scalar gluons in the minimal four color symmetry model,” Mod. Phys. Lett. A **20**, 3003 (2005) [arXiv:hep-ph/0511149].
- [22] I. Dorsner and I. Mocioiu, “Predictions from type II see-saw mechanism in $SU(5)$,” Nucl. Phys. B **796** (2008) 123 [arXiv:0708.3332 [hep-ph]].
- [23] P. Fileviez Perez, R. Gavin, T. McElmurry and F. Petriello, “Grand Unification and Light Color-Octet Scalars at the LHC,” Phys. Rev. D **78** (2008) 115017 [arXiv:0809.2106 [hep-ph]].
- [24] P. Fileviez Perez, H. Iminniyaz and G. Rodrigo, “Proton Stability, Dark Matter and Light Color Octet Scalars in Adjoint $SU(5)$ Unification,” Phys. Rev. D **78** (2008) 015013 [arXiv:0803.4156 [hep-ph]].

- [25] P. Fileviez Perez and M. B. Wise, “On the Origin of Neutrino Masses,” arXiv:0906.2950 [hep-ph].
- [26] P. H. Frampton and S. L. Glashow, “Chiral Color: An Alternative to the Standard Model,” Phys. Lett. B **190** (1987) 157.
- [27] A. Idilbi, C. Kim and T. Mehen, “Factorization and resummation for single color-octet scalar production at the LHC,” arXiv:0903.3668 [hep-ph].
- [28] M. Gerbush, T. J. Khoo, D. J. Phalen, A. Pierce and D. Tucker-Smith, “Color-octet scalars at the LHC,” Phys. Rev. D **77** (2008) 095003 [arXiv:0710.3133 [hep-ph]].
- [29] C. P. Burgess, S. Godfrey, H. Konig, D. London and I. Maksymyk, “A Global fit to extended oblique parameters,” Phys. Lett. B **326** (1994) 276 [arXiv:hep-ph/9307337].
- [30] I. Maksymyk, C. P. Burgess and D. London, “Beyond S, T and U,” Phys. Rev. D **50** (1994) 529 [arXiv:hep-ph/9306267].
- [31] B. Holdom and J. Terning, “Large corrections to electroweak parameters in technicolor theories,” Phys. Lett. B **247** (1990) 88, M. E. Peskin and T. Takeuchi, Phys. Rev. Lett. **65**, 964 (1990). M. Golden and L. Randall, Nucl. Phys. B **361**(1991)3,
- [32] M. E. Peskin and T. Takeuchi, Phys. Rev. D **46** (1992) 381.
- [33] G. Altarelli and R. Barbieri, Phys. Lett. B **253** (1991) 161. G. Altarelli, R. Barbieri and S. Jadach, Nucl. Phys. B **369** (1992) 3 [Erratum-ibid. B **376** (1992) 444].
- [34] M. B. Einhorn, D. R. T. Jones and M. J. G. Veltman, Nucl. Phys. B **191**, 146 (1981).
- [35] M. E. Peskin and J. D. Wells, “How can a heavy Higgs boson be consistent with the precision electroweak measurements?,” Phys. Rev. D **64**, 093003 (2001) [arXiv:hep-ph/0101342].
- [36] P. H. Chankowski, T. Farris, B. Grzadkowski, J. F. Gunion, J. Kalinowski and M. Krawczyk, “Do precision electroweak constraints guarantee $e^+ e^-$ collider discovery of at least one Higgs boson of a two Higgs doublet model?,” Phys. Lett. B **496** (2000) 195 [arXiv:hep-ph/0009271].
- [37] R. Barbieri, L. J. Hall and V. S. Rychkov, “Improved naturalness with a heavy Higgs: An alternative road to LHC physics,” Phys. Rev. D **74**, 015007 (2006) [arXiv:hep-ph/0603188].
- [38] N. G. Deshpande and E. Ma, “Pattern Of Symmetry Breaking With Two Higgs Doublets,” Phys. Rev. D **18**, 2574 (1978).
- [39] C. Amsler et al. (Particle Data Group), Physics Letters B667, 1 (2008)
- [40] M. I. Gresham and M. B. Wise, “Color Octet Scalar Production at the LHC,” Phys. Rev. D **76** (2007) 075003 [arXiv:0706.0909 [hep-ph]].
- [41] C. Kim and T. Mehen, “Color Octet Scalar Bound States at the LHC,” arXiv:0812.0307 [hep-ph].
- [42] J. D. Wells, “TASI lecture notes: Introduction to precision electroweak analysis,” arXiv:hep-ph/0512342.
- [43] M. Pospelov and M. Trott, “R-parity preserving super-WIMP decays,” JHEP **0904**, 044 (2009) [arXiv:0812.0432 [hep-ph]].

- [44] The CDF Collaboration, "Search for Higgs Boson Produced in Association with b-Quarks", CDF Note 8954 v1.0
- [45] T. Aaltonen *et al.* [CDF Collaboration], "Search for new particles decaying into dijets in proton-antiproton collisions at $\sqrt{s} = 1.96$ TeV," arXiv:0812.4036 [hep-ex].
- [46] V. M. Abazov *et al.* [D0 Collaboration], Phys. Lett. B **668**, 98 (2008) [arXiv:0804.3664 [hep-ex]].
- [47] O. Antunano, J. H. Kuhn and G. Rodrigo, "Top quarks, axiguons and charge asymmetries at hadron colliders," Phys. Rev. D **77** (2008) 014003 [arXiv:0709.1652 [hep-ph]].
- [48] T. Aaltonen *et al.* [CDF Collaboration], "Forward-Backward Asymmetry in Top Quark Production in $p\bar{p}$ Collisions at $\sqrt{s} = 1.96$ TeV," Phys. Rev. Lett. **101**, 202001 (2008) [arXiv:0806.2472 [hep-ex]].
- [49] The CDF Collaboration, "Measurement of the Forward-Backward Asymmetry in $t\bar{t}$ Production in $3.2fb^{-1}$ of $p\bar{p}$ collisions at $\sqrt{s} = 1.96$ TeV", CDF Note 9724 v1.0
- [50] The D0 Collaboration, "Search for the Standard Model Higgs Boson in $\gamma\gamma$ final states at D0 with $L = 4.2fb^{-1}$ data", D0 Note 5858-CONF
- [51] V. M. Abazov *et al.* [D0 Collaboration], "Search for the standard model Higgs boson in diphoton final states with the D0 detector," arXiv:0901.1887 [hep-ex].
- [52] G. Buchalla, A. J. Buras and M. E. Lautenbacher, Rev. Mod. Phys. **68**, 1125 (1996) [arXiv:hep-ph/9512380].
- [53] V. Lubicz and C. Tarantino, Nuovo Cim. **123B**, 674 (2008) [arXiv:0807.4605 [hep-lat]].
- [54] A. V. Manohar and M. B. Wise, "Modifications to the properties of a light Higgs boson," Phys. Lett. B **636**, 107 (2006) [arXiv:hep-ph/0601212].
- [55] S. Mantry, M. Trott and M. B. Wise, "The Higgs decay width in multi-scalar doublet models," Phys. Rev. D **77**, 013006 (2008) [arXiv:0709.1505 [hep-ph]].
- [56] S. Mantry, M. J. Ramsey-Musolf and M. Trott, "New Physics Effects in Higgs Decay to Tau Leptons," Phys. Lett. B **660**, 54 (2008) [arXiv:0707.3152 [hep-ph]].
- [57] C. Arnesen, I. Z. Rothstein and J. Zupan, "Smoking Guns for On-Shell New Physics at the LHC," arXiv:0809.1429 [hep-ph].
- [58] N. N. Bogoliubov and O. S. Parasiuk, Acta Math. **97**, 227 (1957).